JACS
JOURNAL OF THE AMERICAN CHEMICAL SOCIETY
Article
pubs.acs.org/JACS

# Identification of a Cyclic Nucleotide as a Cryptic Intermediate in Molybdenum Cofactor Biosynthesis

Bradley M. Hover,[†] Anna Loksztejn,[†] Anthony A. Ribeiro,[‡] and Kenichi Yokoyama*[,†]

[†]Department of Biochemistry, [‡]Duke NMR Spectroscopy Center, and Department of Radiology, Duke University Medical Center, Durham, North Carolina 27710, United States

Supporting Information

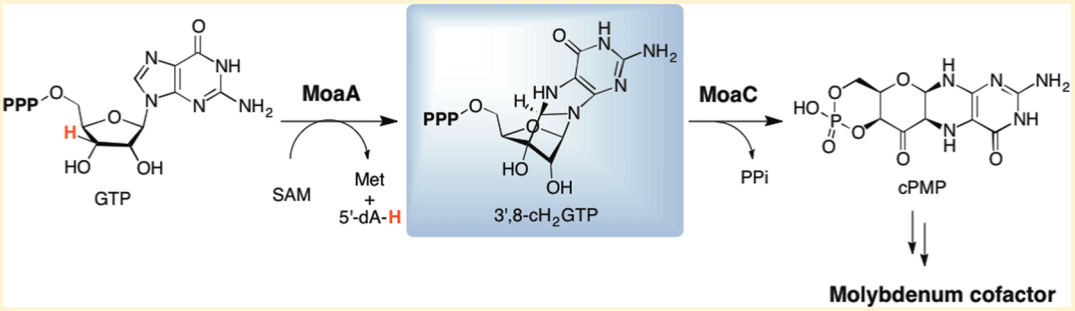


**ABSTRACT:** The molybdenum cofactor (Moco) is a redox cofactor found in all kingdoms of life, and its biosynthesis is essential for survival of many organisms, including humans. The first step of Moco biosynthesis is a unique transformation of guanosine 5′-triphosphate (GTP) into cyclic pyranopterin monophosphate (cPMP). In bacteria, MoaA and MoaC catalyze this transformation, although the specific functions of these enzymes were not fully understood. Here, we report the first isolation and structural characterization of a product of MoaA. This molecule was isolated under anaerobic conditions from a solution of MoaA incubated with GTP, *S*-adenosyl-L-methionine, and sodium dithionite in the absence of MoaC. Structural characterization by chemical derivatization, MS, and NMR spectroscopy suggested the structure of this molecule to be (8*S*)-3′,8-cyclo-7,8-dihydroguanosine 5′-triphosphate (3′,8-cH$_2$GTP). The isolated 3′,8-cH$_2$GTP was converted to cPMP by MoaC or its human homologue, MOCS1B, with high specificities ($K_m$ < 0.060 $\mu$M and 0.79 ± 0.24 $\mu$M for MoaC and MOCS1B, respectively), suggesting the physiological relevance of 3′,8-cH$_2$GTP. These observations, in combination with some mechanistic studies of MoaA, unambiguously demonstrate that MoaA catalyzes a unique radical C−C bond formation reaction and that, in contrast to previous proposals, MoaC plays a major role in the complex rearrangement to generate the pyranopterin ring.

## INTRODUCTION

The molybdenum cofactor (Moco, **5**, Figure 1a) is a redox cofactor found in almost all organisms.[1,2] Moco-dependent enzymes play central roles in many biologically important processes such as purine and sulfur catabolism in mammals, anaerobic respiration in bacteria, and nitrate assimilation in plants.[2] In humans, Moco deficiency results in the pleiotropic loss of all molybdenum enzyme activities, causing neurological abnormalities and early childhood death.[3,4] Unlike many other cofactors, Moco cannot be taken up as a nutrient, and thus it requires *de novo* biosynthesis. Moco biosynthesis (Figure 1a) is thought to be conserved among all organisms[5,6] and initiated by the conversion of guanosine 5′-triphosphate (GTP, **1**) into cyclic pyranopterin monophosphate (cPMP, **3**).[7−9] cPMP is then converted to Moco by the introduction of two sulfur atoms[10−12] and a molybdate.[13−16]

Previous isotope tracer experiments indicated that the conversion of GTP to cPMP proceeds through the insertion of C-8 of guanine between C-2′ and C-3′ of ribose (Figure 1a).[7,17] This contrasts with the biosynthesis of pterin rings in other GTP-derived cofactors such as folate and flavins, in which C-8 of GTP is released as a formate during the reaction catalyzed by GTP cyclohydrolases (Figure S1a).[18,19] Thus, the retention of GTP C-8 in Moco biosynthesis indicated a novel mechanism of pterin ring formation.

Two enzymes, MoaA and MoaC in bacteria, are responsible for the conversion of GTP to cPMP.[7,9,20,21] Bioinformatic analysis suggested that MoaA belongs to the radical *S*-adenosyl-L-methionine (SAM) superfamily.[22] Enzymes in this superfamily catalyze the reductive cleavage of SAM using an oxygen-labile [4Fe-4S] cluster as a reductant, and transiently generate a 5′-deoxyadenosyl radical (5′-dA$^•$), which then abstracts a H-atom from substrate to initiate radical reactions.[23] The classification of MoaA as a radical SAM enzyme was supported by an *in vitro* activity assay of MoaA in the presence of MoaC, in which the conversion of GTP into cPMP requires the presence of SAM.[9] The X-ray crystal structures of *Staphylococcus aureus* MoaA[9] revealed the binding of SAM to a [4Fe-4S] cluster, in a fashion similar to other radical SAM

**Received:** February 18, 2013
**Published:** April 29, 2013

  

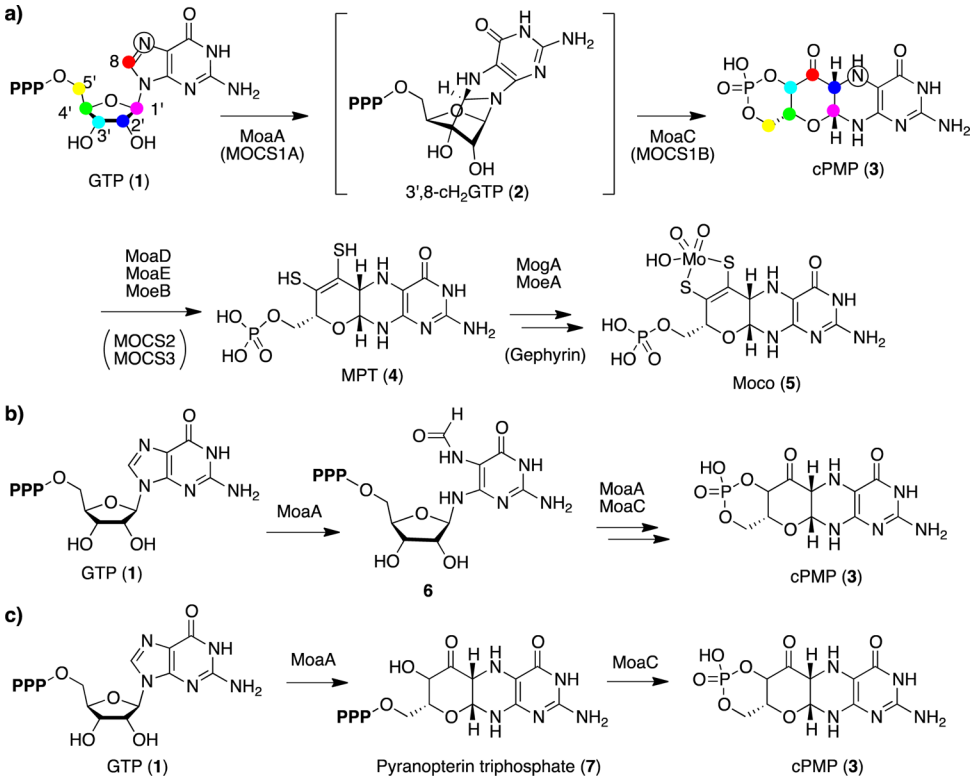


**Figure 1.** (a) Moco biosynthetic pathway in bacteria and humans. The human enzymes are indicated in parentheses. The symbols on GTP and cPMP indicate the source of the carbon and nitrogen atoms in cPMP as determined by isotope labeling studies.[7,17] **P** designates a phosphate group. 3′,8-cH$_2$GTP is shown in brackets, as it had not been identified prior to this report. (b) Previous proposal for the functions of MoaA and MoaC with 2-amino-5-formylamino-6-ribofuranosylamino-4-pyrimidinone triphosphate (**6**) as an intermediate.[29,33] (c) Previous proposal for the functions of MoaA and MoaC by Mehta et al.[30] Pyranopterin triphosphate 7 was proposed as the product of MoaA.

enzymes.[24,25] The structure also revealed the presence of an additional C-terminal [4Fe-4S] cluster. This C-terminal [4Fe-4S] cluster was shown to bind various purine nucleoside 5′-triphosphates including GTP on the basis of equilibrium dialysis and X-ray crystallography,[26] as well as electron−nuclear double-resonance (ENDOR) spectroscopy.[27] Together with the reported binding constant (0.29 $\mu$M),[26] GTP was proposed as a substrate of MoaA.

Many radical SAM enzymes are known to catalyze complex rearrangement reactions.[23,28] MoaA has also been considered to catalyze the majority, if not all, of the complex rearrangement of GTP to form the pyranopterin ring of cPMP.[5,6,29,30] Schindelin and Hänzelmann first proposed that, in the absence of MoaC, purified MoaA catalyzes conversion of GTP into a molecule with a 6-hydroxy-2,4,5-triaminopyrimidine partial structure, on the basis of the chemical derivatization to dimethylpterin (DMPT).[26] Unfortunately, no data were presented. This observation was analogous to those for folate biosynthesis, where the imidazole moiety of guanine base in GTP is first hydrolyzed to a 2-amino-5-formylamino-6-ribofuranosylamino-4-pyrimidinone triphosphate (Figure S1a),[31] which may be chemically derivatized to DMPT (Figure S1b). This analogy has prompted speculations about the reaction catalyzed by MoaA,[29,32] which consider 2-amino-5-formylamino-6-ribofuranosylamino-4-pyrimidinone triphosphate (**6**) as an intermediate or a product of the MoaA-catalyzed reaction (Figure 1b).

Recently, a more definitive proposal for the product of MoaA was made by Mehta et al.[30] In their report, the authors performed LC-MS analysis of small molecules produced after incubation of MoaA with GTP, SAM, and dithionite in the absence of MoaC, in which a molecule with light absorption at 320 nm and a mass signal at $m/z$ = 524 $[M+H]^+$ was observed. Reactions using series of deuterated GTP suggested that a deuterium at the 3′ position of GTP is transferred to 5′-deoxyadenosine (5′-dA) produced in this assay. However, the observed putative MoaA product was not isolated for further structural characterization, and the relation of this observation to the earlier one by Schindelin and Hänzelmann[26] was not discussed. It is currently unknown whether the putative MoaA product could serve as a substrate of MoaC and be converted to cPMP. Nevertheless, on the basis of these observations, the authors proposed that MoaA catalyzes conversion of GTP into pyranopterin triphosphate (**7**, Figure 1c).[30]

The role of MoaC, on the other hand, has been significantly under-appreciated. MoaC does not show significant amino acid sequence similarities to functionally characterized proteins. Currently, structures of MoaC from four different organisms have been reported.[32−35] A putative ligand binding site was proposed on the basis of the conservation of amino acid residues and their relative positions in a crystal structure.[34] A structure of MoaC from *Thermus thermophilus* in combination with isothermal titration calorimetry experiments suggested that nucleotide triphosphate may bind to the putative ligand binding site.[33] In the recent publication by Mehta et al.,[30] MoaC was proposed to be responsible only for the formation of the cyclic phosphate (Figure 1c) on the basis of their premise that the MoaA product is pyranopterin triphosphate. However, uncertainty remains about the relevance of this proposal due to the limited characterization of the MoaA reaction product.


dx.doi.org/10.1021/ja401781t | *J. Am. Chem. Soc.* 2013, 135, 7019−7032

In the current study, we report the isolation and detailed characterization of the MoaA reaction product, which unambiguously delineated the individual reactions catalyzed by MoaA and MoaC. Isolation of the MoaA reaction product was achieved under anaerobic conditions with careful control of pH. Structural characterization by chemical derivatization, MS, and NMR spectroscopy established the structure of this molecule as (8*S*)-3′,8-cyclo-7,8-dihydroguanosine 5′-triphosphate (3′,8-cH$_2$GTP, **2**). The relevance of the isolated 3′,8-cH$_2$GTP as a physiological Moco biosynthetic intermediate was demonstrated by steady-state kinetic analysis of MoaC and its human homologue, MOCS1B. MoaC and MOCS1B converted 3′,8-cH$_2$GTP to cPMP with $K_m$ values of <0.06 and 0.79 $\mu$M, respectively. Additional studies on the stoichiometry of the MoaA reaction in combination with an isotope tracer experiment suggest that the conversion of GTP to 3′,8-cH$_2$GTP proceeds through H-abstraction from the 3′ position by consuming a stoichiometric amount of SAM. The observations presented here in sum unequivocally delineate the individual functions of MoaA and MoaC and provide insights into the biosynthesis of cPMP. The current identification of 3′,8-cH$_2$GTP as a substrate of MoaC is a sharp contrast to previous proposals,[29,30] in which MoaC was thought to have minimal or no function in the formation of the pyranopterin structure. These results provide a basis for future mechanistic studies of reactions catalyzed by these two enzymes.

## MATERIALS AND METHODS

QAE A25 Sephadex resin, guanosine 5′-triphosphate (GTP), [U-$^{13}C_5$,$^{15}N_{10}$]GTP, *S*-adenosyl-L-methionine (SAM), 5′-deoxyadenosine (5′-dA), dithiothreitol (DTT), sodium dithionite, 2,3-butanedione, and dimethylpterin (DMPT) were purchased from Sigma-Aldrich. DEAE sepharose FF resin was from GE Healthcare. [3-$^2$H]Ribose was from Omicron Biochemicals Inc. Chemically competent *Escherichia coli* DH5$\alpha$ and BL21(DE3) cells and all PCR primers were from Invitrogen. pET expression plasmids were from Novagen. Calf-intestine alkaline phosphatase (CIAP, 20 U/$\mu$L) was from NEB. UV−vis absorption spectra were determined using a U-3900 UV−vis ratio-recording double-beam spectrometer (Hitachi) or a Nanodrop 1000 instrument (Thermo Scientific). Nonlinear least-squares fitting of kinetic data was carried out using KaleidaGraph software (Synergy Software, Reading, PA). Anaerobic experiments were carried out in a UNIlab workstation glovebox (MBaun, Stratham, NH) maintained at 10 ± 2 °C with $O_2$ concentration <0.1 ppm. All anaerobic solutions were degassed on a Schlenk line and equilibrated in the glovebox atmosphere for >12 h. All plastic devices for anaerobic use were evacuated for >12 h in the glovebox antechamber before being brought into the glovebox. All DNA sequences were confirmed by Eton Bioscience Inc. PCR was carried out using PfuUltraII polymerase (Stratagene) according to the manufacturer's protocol. All HPLC experiments were performed on a Hitachi L-2130 pump equipped with an L-2455 diode array detector, an L-2485 fluorescence detector, an L-2200 autosampler, and an ODS Hypersil C18 column (Thermo Scientific) housed in an L-2300 column oven maintained at 40 °C. *S. aureus* MoaA and MoaC were expressed and purified by published protocols[9] with minor modification as described in the Supporting Information. The expression plasmids for SUF proteins[36] and MOCS1B[37] were kindly provided by Dr. Herman Schindelin. The 5-methylthioribose kinase expression plasmid[38] was a generous gift from Dr. John Gerlt.

**Stepwise Assay of MoaA and MoaC.** The stepwise MoaA/MoaC assays were carried out under anaerobic conditions. First, MoaA (5 $\mu$M) was incubated with GTP (1 mM), SAM (1 mM), and sodium dithionite (1 mM) in 200 $\mu$L of assay buffer (50 mM Tris-HCl, pH 7.6, 1 mM $MgCl_2$, 2 mM DTT, and 0.3 M NaCl). The reaction was initiated by the addition of MoaA and incubated for 60 min at 25 °C, at which point MoaA was removed by ultrafiltration (Amicon Ultra 30 K, Millipore). To an aliquot (80 $\mu$L) of the resulting small-molecule fraction, 10 $\mu$L of 50 $\mu$M MoaC was added and incubated for 60 min at 25 °C. The reaction was stopped by addition of 10 $\mu$L of 25% (w/v) trichloroacetic acid (TCA). cPMP formed during the incubation with MoaC was oxidized to compound Z and quantified by HPLC following the published protocol.[7] Briefly, a solution (10 $\mu$L) containing 1% (w/v) $I_2$ and 2% (w/v) KI was added to the quenched reaction mixture and incubated for 20 min at room temperature. After removal of precipitate by centrifugation, an aliquot (10 $\mu$L) of the supernatant was injected to the HPLC. Chromatography was performed by an isocratic elution with 0.1% TFA in $H_2O$ with a flow rate of 1 mL/min and monitored by fluorescence (excitation 367 nm, emission 450 nm). Under these conditions, the void volume was 1.5 min, and compound Z eluted at 2.7 min. The authentic compound Z standard was isolated from Δ*MoeB E. coli* strain by following the reported protocol.[8]

**Detection of the MoaA Product as DMPT.** MoaA (5 $\mu$M) was incubated with GTP (1 mM), SAM (1 mM), and sodium dithionite (1 mM) in assay buffer (0.5 mL). The reaction was initiated by the addition of MoaA and incubated at 25 °C for a specified time. An aliquot (80 $\mu$L) was removed at each time point and mixed with 10 $\mu$L of 0.5 M HCl to quench the reaction. The resulting mixture was incubated at 95 °C for 5 min to facilitate the hydrolysis, followed by addition of 6 $\mu$L of 1 M NaOH to adjust the pH to 8.5. The resulting solution was combined with 25 $\mu$L of 0.66% (v/v) 2,3-butanedione solution in 0.9 M Tris-HCl, pH 8.5, and incubated at 95 °C for 45 min. After removal of precipitate by centrifugation, an aliquot (10 $\mu$L) of the supernatant was injected to the HPLC. Chromatography was performed by an isocratic elution with 92.5% 20 mM sodium acetate, pH 6.0, and 7.5% MeOH with a flow rate of 1 mL/min and monitored by fluorescence (excitation 365 nm, emission 445 nm). Under these conditions, the void volume was 1.5 min, and DMPT eluted at 5.6 min.

**3′,8-cH$_2$GTP Stability Test.** The temperature and pH stabilities were assessed by incubating 3′,8-cH$_2$GTP (50 $\mu$M) solution in anaerobic buffer (15 mM ammonium formate, pH 3.5, 50 mM Tris-HCl, pH 7.6, or 15 mM ammonium bicarbonate, pH 9.0) in the glovebox at 10 or 22 °C. To test for oxygen sensitivity, 3′,8-cH$_2$GTP (50 $\mu$M) solution was taken out of the glovebox and exposed to air by rigorous pipetting. For each reaction, an aliquot (10 $\mu$L) was removed at specified time points and incubated with MoaC in 80 $\mu$L of assay buffer (50 mM Tris-HCl, pH 7.6, 0.3 M NaCl, 1 mM $MgCl_2$, and 2 mM DTT). The reaction was quenched with 10 $\mu$L of 25% TCA, and cPMP was quantified as described above for the stepwise assay.

**Isolation of 3′,8-cH$_2$GTP.** The MoaA reaction and subsequent purification of 3′,8-cH$_2$GTP were carried out under strict anaerobic conditions (<0.1 ppm $O_2$). The large-scale MoaA reaction for the isolation of 3′,8-cH$_2$GTP was carried out with MoaA (200 $\mu$M), SAM (1 mM), sodium dithionite (1 mM), and GTP or [U-$^{13}C_5$,$^{15}N_{10}$]GTP (200 $\mu$M) in 50 mM Tris-HCl, pH 7.6 (200 mL), at 22 °C for 60 min. These reactions typically produced 12−20 $\mu$mol of 3′,8-cH$_2$GTP. Subsequent purification was carried out at 10 °C. The MoaA reaction mixture was first passed through an ultrafiltration membrane (Amicon YM-30, Millipore) to remove the protein, and the resulting filtrate was applied to a QAE A25 Sephadex (250 mL, bicarbonate form) column. The column was washed with 750 mL of $H_2O$, and elution was performed by a linear gradient (600 × 600 mL) of 200−800 mM ammonium bicarbonate, pH 9.1. To identify the fractions containing 3′,8-cH$_2$GTP, an aliquot (10 $\mu$L) of each fraction was mixed with 80 $\mu$L of MoaC (20 $\mu$M) in assay buffer and incubated for 30 min at 25 °C. The resulting solutions were analyzed for cPMP as described above for the stepwise assay. The fractions containing 3′,8-cH$_2$GTP were combined, lyophilized, re-dissolved in water, and applied to a DEAE sepharose FF (15 mL, bicarbonate form) column. The column was washed with 50 mL of 100 mM ammonium bicarbonate, pH 9.1, and eluted by a linear gradient (300 × 300 mL) of 100−200 mM ammonium bicarbonate, pH 9.1. The fractions containing 3′,8-cH$_2$GTP were identified by UV−vis absorption spectroscopy and


dx.doi.org/10.1021/ja401781t | J. Am. Chem. Soc. 2013, 135, 7019−7032

the MoaC activity assay described above. After removal of the solvent by lyophilization, the purified 3′,8-cH$_2$GTP was characterized by NMR and ESI-TOF-MS.

**Phosphate Quantitation.** Phosphate quantitation was carried out on the basis of the published protocol.[8,39] Purified 3′,8-cH$_2$GTP (4 pmol) was incubated with CIP (5 units; each unit is defined as the amount of enzyme that hydrolyzes 1 nmol of *p*-nitrophenylphosphate per minute at 37 °C) for 1 h at 37 °C in 100 μL of 50 mM Tris-HCl, pH 7.9, containing 100 mM NaCl, 10 mM $MgCl_2$, and 1 mM DTT. The resulting solution was then mixed with 0.233 mL of 1.4% (w/v) ascorbic acid and 0.36% (w/v) ammonium molybdate tetrahydrate in 0.86 M $H_2SO_4$. After an hour of incubation at 37 °C, the phosphate concentration was determined on the basis of the absorption of the phosphomolybdate complex at 820 nm ($\varepsilon_{820nm}$ = 26.0 $mM^{-1}$ $cm^{-1}$).[39]

**Determination of the Molecular Weight of 3′,8-cH$_2$GTP.** Purified 3′,8-cH$_2$GTP (100 μM) in anaerobic water was prepared in the glovebox. An aliquot (10 μL) of the sample was injected into the ESI-TOF MS instrument (Agilent 6224) operated in the negative ion mode. The typical mass accuracy of the instrument was 5 ppm. For the characterization of the observed MS signal, 3′,8-cH$_2$GTP (100 μM) was anaerobically incubated with MoaC (50 μM) in 400 μL of 300 mM ammonium bicarbonate buffer, pH 9.1, for 20 min at 25 °C. After removal of MoaC by ultrafiltration (Amicon YM-10, Millipore), the solution was lyophilized, and the residue was dissolved in 400 μL of anaerobic water. The resulting solution was analyzed by ESI-TOF MS as described for 3′,8-cH$_2$GTP.

**NMR Measurements of Purified 3′,8-cH$_2$GTP.** All NMR spectra were recorded on 500, 600, or 800 MHz Varian Inova NMR spectrometers operated with VNMRJ 3.1 software and analyzed by the ACD/NMR processor (ACD/Laboratories). The samples were dissolved in anaerobic deuterium oxide (Sigma-Aldrich, 99.9 atom% enriched), loaded in 3 mm NMR tubes (Wilmad LabGlass) in the glovebox, and sealed with butyl rubber septa (Sigma-Aldrich). NMR measurements were carried out for 24−48 h at a sample temperature of 6 °C. No decomposition of 3′,8-cH$_2$GTP was observed during the NMR measurements based on a comparison of $^1$H NMR spectra at the beginning and the end of the measurements. Chemical shifts are reported in $\delta$ based on an internal standard, 4,4-dimethyl-4-silapentane-1-sulfonic acid (DSS, $\delta_{CH_3}$ = 0.00) as reference. Maleic acid ($\delta_{CH}$ = 6.0, Sigma-Aldrich) was used as an internal standard for signal quantitation.

**MoaA/C Coupled Assay.** Enzyme activity assays were performed at 25 °C under anaerobic conditions by incubating MoaA (0.5 μM) and MoaC (5 μM) with GTP (1 mM), SAM (1 mM), and sodium dithionite (1 mM) in assay buffer. The reaction was initiated by the addition of MoaA. At each time point, an aliquot (90 μL) was removed and mixed with 10 μL of 25% (w/v) TCA to quench the reaction. cPMP was quantified as described above for the stepwise assay.

**Preparation of MOCS1B Expression Plasmid.** The *MOCS1B* gene in the pQE-MOCS1B plasmid originally prepared by Hänzelmann et al.[37] was subcloned into pET-28b to improve protein expression. *Nde*I restriction site was introduced by PCR at the 5′ end of the *MOCS1B* gene in the pQE-MOCS1B plasmid using primers MOCS1B-f (CAT CAC CAT CAC CAT ATGATG AGT TTC TC) and MOCS1B-r (GAG AAA CTC ATC ATA TGG TGA TGG TGA TG). After confirmation of the DNA sequence, the resulting plasmid was digested with *Nde*I and *Sal*I, and the *MOCS1B* gene fragment was subcloned into the corresponding site of pET28b to obtain pET-MOCS1B.

**Expression of MOCS1B.** *E. coli* BL21(DE3) cells were co-transformed with pET-MOCS1B and grown overnight on LB agar plates. All growths were carried out in the presence of kanamycin (50 mg/L). A single colony was picked and grown in LB medium (5 mL) to saturation (~16 h). Two milliliters of this solution was diluted into 200 mL of LB medium in a 500 mL baffled flask and incubated at 37 °C until growth reached saturation. A portion of this culture (10 mL) was then used to inoculate 1.5 L of 2YT medium in a 2.8 L baffled flask and grown at 37 °C until $OD_{600}$ reached 0.6−0.8, at which time the temperature was lowered to 15 °C and MOCS1B expression was induced with 0.3 mM IPTG. The culture was continued for an additional 20 h until saturation, and cells were harvested by centrifugation, frozen in liquid $N_2$, and stored at −80 °C. Typically, 10 g of wet cell paste per liter was obtained.

**Purification of MOCS1B.** The cell paste (10 g) of *E. coli* BL21(DE3) expressing MOCS1B was suspended in 50 mL of buffer A (50 mM Tris-HCl, pH 9.0, 0.3 M NaCl, 10% glycerol) supplemented with 1% Triton-X and a protease inhibitor cocktail (Calbiochem no. 539132). The cell suspension was homogenized and lysed by two passages through a French pressure cell operating at 14 000 psi. After removal of cell debris by centrifugation (20000*g*, 20 min, 4 °C), DNA was precipitated by dropwise addition of 0.2 vol of buffer A containing 8% (w/v) streptomycin sulfate. The mixture was stirred for an additional 15 min, and the precipitated DNA was removed by centrifugation (20000*g*, 20 min, 4 °C). Solid $(NH_4)_2SO_4$ (0.23 g per mL) was then added over 15 min to 40% saturation. The solution was stirred for an additional 20 min, and the precipitated protein was isolated by centrifugation (20 000*g*, 20 min, 4 °C). The protein pellet was dissolved in a minimal volume of buffer A supplemented with 1% Triton-X, 0.5 mM phenylmethanesulfonyl fluoride (PMSF), and 20 mM imidazole and applied to a Ni-NTA column (10 mL). The column was then washed with 10 vol of the same buffer, followed by another 10 vol of buffer A containing 20 mM imidazole. MOCS1B was subsequently eluted with 500 mM imidazole in buffer A. Fractions containing MOCS1B were identified by SDS-PAGE, combined, and exchanged into buffer A on a Sephadex G-25 column. The resulting MOCS1B was concentrated by ultrafiltration (Amicon Ultra 3 K, Millipore) to 0.2 mM, flash frozen in liquid nitrogen, and stored at −80 °C. The concentration of MOCS1B was determined on the basis of UV absorption at 280 nm using an extinction coefficient ($\varepsilon_{280nm}$ = 15.9 $mM^{-1}$ $cm^{-1}$) determined by Edelhoch's method.[40] To characterize the three MOCS1B polypeptides, each polypeptide was purified on SDS-PAGE and digested with L-1-tosylamido-2-phenylethyl chloromethyl ketone-treated Porcin trypsin (Promega). The resulting tryptic peptides were analyzed by LC-MS at the Duke proteomics core facility.

**Activity Assays of MoaC and MOCS1B.** MoaC (0.1 μM) or MOCS1B (0.5 μM) was anaerobically incubated with 3′,8-cH$_2$GTP at specified concentrations in assay buffer at 25 °C. The reaction was initiated by the addition of MoaC or MOCS1B, and an aliquot (90 μL) was removed at each time point and mixed with 10 μL of 25% (w/v) TCA to quench the reaction. cPMP was quantified as described above for the stepwise assay.

**Quantitation of 5′-dA.** Enzyme reactions were performed and quenched as described for the MoaA/C coupled assay except that 20 μM MoaA and 40 μM MoaC were used. After the TCA quenching, the solution was clarified by centrifugation, and an aliquot (70 μL) of the supernatant was injected to HPLC. Chromatography was performed by a linear gradient of 0−15% MeOH in 27 mM $KH_2PO_4$, pH 4.5 (25 min, 2 mL/min), and monitored by UV absorption at 256 nm.

**Preparation of [3′-$^2$H]GTP.** *Enzymatic Synthesis of [3′-$^2$H]-Guanosine.* [3-$^2$H]Ribose (1 mM, > 95% enriched) was incubated at 27 °C with ATP (2 mM), guanine (2 mM), 5-methylthioribose kinase (3.5 μM),[38] and purine nucleoside phosphorylase (Sigma-Aldrich, 3.5 μM) in 200 mL of 10 mM Tris-HCl, pH 7.6, containing 2.5 mM $MgCl_2$ and 2.5 mM DTT. After 2 h of incubation at 27 °C, the solution was adjusted to pH 3 with 1 M HCl and loaded on to a Dowex 50W-X8 column (2 × 10 cm, ammonium form). The column was washed with 15 mM ammonium formate, pH 3.0, and eluted with 300 mM ammonium formate, pH 9.0. Fractions containing guanosine were identified by UV−vis absorption and thin-layer chromatography. Guanosine was typically eluted after 7−10 column volumes of elution. The fractions containing guanosine were combined, and the solvent was removed by lyophilization to yield 100 μmol of [3′-$^2$H]guanosine (94 ± 3 atom% $^2$H): $^1$H NMR (500 MHz, $D_2O$) $\delta$ 7.95 (s, 1 H), 5.86 (d, $J$ = 7.3 Hz, 1 H), 4.62 (m, 1H), 4.18 (br, 1 H), 3.84 (dd, $J$ = 2.9, 12.7 Hz, 1H), 3.77 (dd, $J$ = 3.9, 12.7 Hz, 1H); HRMS (ESI-TOF) $m/z$ $[M+H]^+$ calcd for $C_{10}H_{13}DN_5O_5$ 285.106, found 285.107.

*Phosphorylation of [3′-$^2$H]Guanosine.* Phosphorylation of guanosine was performed by the Ludwig's method.[41] Briefly, [3′-$^2$H]-

guanosine (100 $\mu$mol) was dried by co-evaporation with dry pyridine and dissolved in dry $(MeO)_3PO$ (1.5 mL). To this solution was added $POCl_3$ (130 $\mu$mol), and the mixture was stirred on ice for 2 h. Bis-tri-*n*-butylammonium pyrophosphate (500 $\mu$mol) in anhydrous DMF (2 mL) and $Bu_3N$ (100 $\mu$L) was then added under rigorous stirring. After 10 min, 7 mL of 1 M triethylammonium bicarbonate, pH 7.5, was poured into the solution and stirred for 15 min. The resulting mixture was diluted by 5-fold with water and applied to QAE A25 Sephadex (Sigma, 4 × 20 cm, bicarbonate form). The column was washed with 0.2 M ammonium bicarbonate pH 8.0 (100 mL), and the elution was performed with a linear gradient (450 × 450 mL) of 0.2−1 M ammonium bicarbonate, pH 8.0. GTP was eluted between 0.55 and 0.7 M ammonium bicarbonate, judged by UV−vis absorption. Lyophilization of these fractions yielded 24 $\mu$mol of [3′-$^2$H]GTP (94 ± 3 atom% $^2$H): $^1$H NMR (500 MHz, $D_2O$) $\delta$ 7.92 (s, 1 H), 5.71 (d, $J$ = 5.9 Hz, 1 H), 4.56 (d, $J$ = 5.9 Hz, 1 H), 4.15 (br, 1 H), 4.04 (m, 2 H); $^{31}$P NMR (160 MHz, $D_2O$) $\delta$ −8.04 (br), −11.26 (d, $J$ = 19 Hz), −22.45 (br); HRMS (ESI-TOF) $m/z$ $[M-H]^-$ calcd for $C_{10}H_{14}DN_5O_{14}P_3$ 522.990, found 522.991.

**MoaA Reaction with [3′-$^2$H]GTP and Isolation of [5′-$^2$H]5′-dA.** [3′-$^2$H]GTP (98 $\mu$M) was anaerobically incubated with MoaA (50 $\mu$M), MoaC (100 $\mu$M), SAM (1 mM), and sodium dithionite (1 mM) in assay buffer for 1 h at 25 °C. Proteins were removed by ultrafiltration (Amicon Ultra 30 K, Millipore), and the resulting filtrate was applied to a C18 RP Silica 90 column (Sigma, 2 × 8 cm) equilibrated in water. Elution was performed using a linear gradient (300 × 300 mL) with 0−30% MeOH in water. 5′-dA was eluted at 15% MeOH judged by UV−vis absorption at 256 nm. After removal of the solvent by rotary evaporation, the sample was further purified by HPLC using conditions identical to those described above for the quantitation of 5′-dA, except that 30 mM ammonium formate, pH 4.5, was used as the aqueous solvent. The resulting sample was lyophilized and characterized by $^1$H NMR, $^2$H NMR, and ESI-TOF-MS.

## RESULTS

**Investigation for an Intermediate between GTP and cPMP.** While small molecules produced by MoaA were previously proposed to serve as a substrate of MoaC,[30] the conversion of this molecule to cPMP by MoaC in the absence of MoaA has never been demonstrated. Considering the complexity of the conversion of GTP into cPMP, and enzyme-catalyzed radical reactions in general,[28,42] the absence of such demonstration leaves significant ambiguity about the relevancy of the observations to Moco biosynthesis. Thus, we carried out stepwise activity assays using *S. aureus* MoaA and MoaC. In these assays, GTP (1 mM) was first incubated with MoaA (5 $\mu$M), SAM (1 mM), and sodium dithionite (1 mM) in the absence of MoaC. The resulting small molecules were separated from MoaA by ultrafiltration, and subsequently incubated with MoaC (5.6 $\mu$M). Any cPMP present in the resulting reaction solution was quantified by HPLC analysis after a conversion to its fluorescent derivative, compound Z (**8**, Figure 2a), following the previously established protocol.[8] Figure 2a shows the results of HPLC analysis that shows a peak co-migrating with compound Z. Quantitation of the observed HPLC peak using an authentic standard suggested formation of 3.6 ± 0.3 $\mu$M compound Z, substoichiometric to MoaA. Control reactions lacking GTP or SAM did not yield compound Z. These observations are consistent with the presence of a small molecule intermediate that is produced by MoaA, and converted to cPMP by MoaC.

**Chemical Derivatization of the MoaA Reaction Product.** For the biosynthesis of other pterins and flavins, nucleotide biosynthetic intermediates with a 6-hydroxy-2,4,5-triaminopyrimidine partial structure have been reported (see Figure S1a for the structural formula).[31,43] These nucleotides

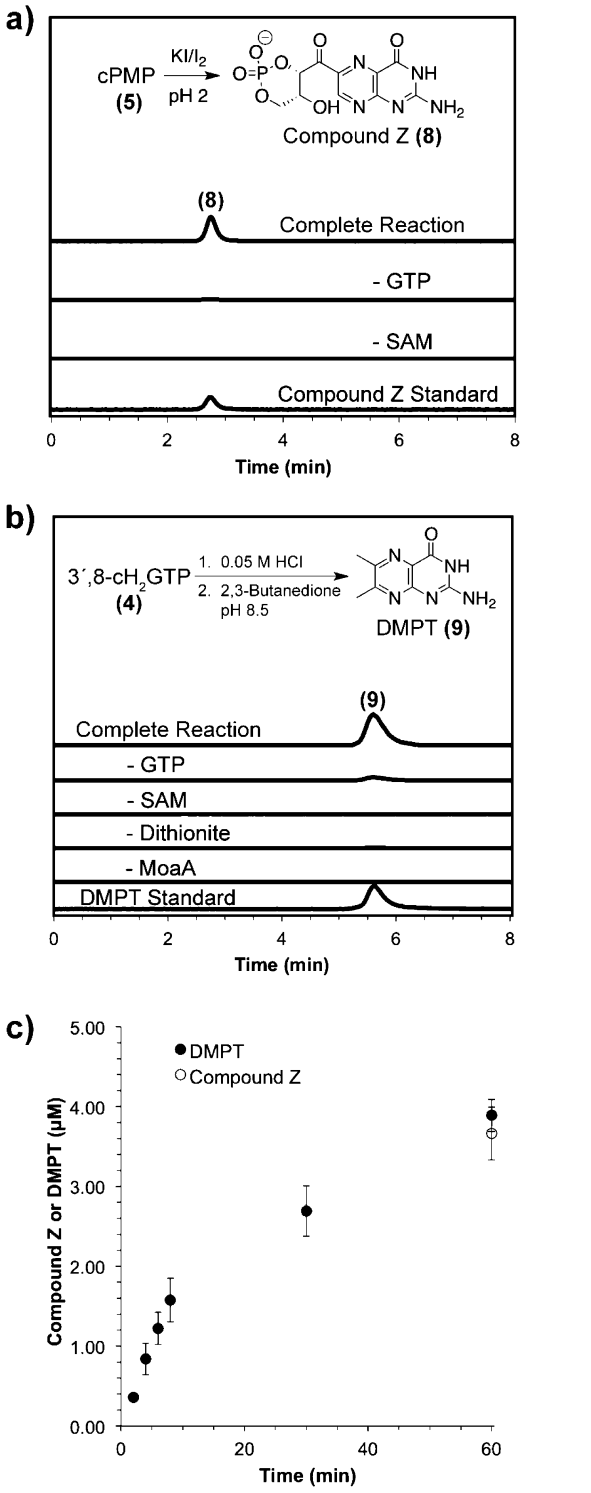


**Figure 2.** Activity assays of MoaA. (a) HPLC analysis of stepwise MoaA/MoaC activity assay (excitation 367 nm, emission 450 nm). In the complete reaction, GTP (1 mM), SAM (1 mM) and sodium dithionite (1 mM) were incubated with MoaA (5 $\mu$M) for 60 min at 25 °C, followed by removal of MoaA by ultrafiltration and incubation with MoaC (15 $\mu$M) for 60 min at 25 °C. cPMP was converted to compound Z (**8**), and detected by HPLC. Also shown are the chromatograms for the compound Z standard, and control reactions without GTP or SAM. (b) HPLC analysis of MoaA activity assay (excitation 365 nm, emission 445 nm). In the complete condition, MoaA (5 $\mu$M), was incubated with GTP (1 mM), SAM (1 mM), and sodium dithionite (1 mM) at 25 °C for 60 min. The reaction product was subjected to acid hydrolysis, followed by incubation with 2,3-


dx.doi.org/10.1021/ja401781t | J. Am. Chem. Soc. 2013, 135, 7019−7032

**Figure** 2. continued

butanedione, and analyzed for the fluorescent DMPT (**9**). Also shown are the chromatograms for the DMPT standard, and for control reactions lacking GTP, SAM, dithionite, or MoaA. A small amount of DMPT (~10% of the complete condition) was formed in the GTP negative control due to the copurification of GTP with MoaA. (c) Time course of 3′,8-cH$_2$GTP formation determined after conversion to DMPT (filled circles) or compound Z (open circle). The conditions for the MoaA reaction and the derivatization of the product to DMPT are identical to (b). The amount of compound Z at 60 min is based on the quantitation of the HPLC peak in (a). Each point is an average of three replicates, and the error bars are calculated on the basis of the standard deviation.

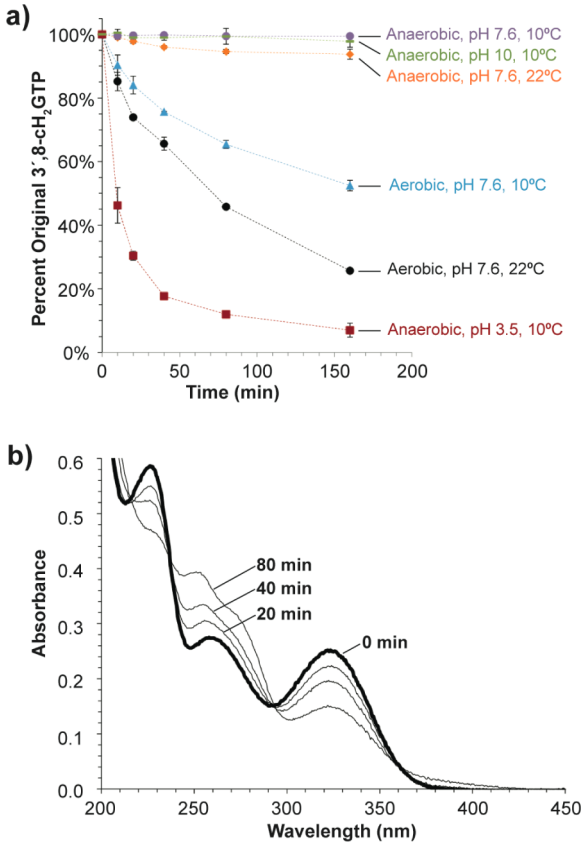


**Figure 3.** (a) Stability of 3′,8-cH$_2$GTP under different conditions. Solution containing 3′,8-cH$_2$GTP was incubated for 10−180 min under specified conditions. At each time point, an aliquot was removed and 3′,8-cH$_2$GTP was quantified by HPLC after its conversion to compound Z. Each point is an average of three replicates, and the error bars are calculated on the basis of the standard deviation. (b) UV−vis absorption spectrum of 3′,8-cH$_2$GTP (bold trace) (50 $\mu$M). The thin traces are spectra after exposure to air at 22 °C for the specified time.

have been characterized by derivatization of a hydrolytically released 6-hydroxy-2,4,5-triaminopyrimidine to the highly fluorescent DMPT (**9**; see Figure S1b for the chemical equation for the derivatization). Schindelin et al. briefly mentioned in their publication[26] that the MoaA reaction product can be converted to DMPT, although no data were presented. We thus attempted a similar derivatization to investigate whether the MoaA product contains an acid-labile 6-hydroxy-2,4,5-triaminopyrimidine partial structure. For this purpose, enzyme activity assays were performed with MoaA (5 $\mu$M), GTP (1 mM), SAM (1 mM), and sodium dithionite (1 mM) under anaerobic conditions in the absence of MoaC. The reaction was stopped by the addition of hydrochloric acid, and the resulting solution was incubated at 95 °C to facilitate hydrolysis, followed by incubation with 2,3-butanedione at pH 8. Figure 2b shows the HPLC analysis of this reaction, which reveals the formation of DMPT. Omission of any of the reaction components resulted in significant decrease of DMPT. The time course assay (Figure 2c) revealed that increasing amounts of DMPT were formed with prolonged incubation time (Figure 2c). The concentration of DMPT observed in this assay at the 60 min time point (3.8 ± 0.2 $\mu$M) was substoichiometric to that of MoaA (5 $\mu$M), and within errors to the amount of cPMP observed in the stepwise assay (3.6 ± 0.3 $\mu$M, compare filled and open circles at 60 min time point in Figure 2c). Together with the results of the stepwise assays, these preliminary characterizations prompted us to attempt isolation of 3′,8-cH$_2$GTP.

**Isolation of 3′,8-cH$_2$GTP.** The isolation of 3′,8-cH$_2$GTP was a significant challenge primarily due to its limited stability. As shown in Figure 3a, decomposition of 3′,8-cH$_2$GTP was observed under aerobic conditions or under acidic pH. This limited stability required all the purifications to be carried out in an anaerobic glovebox ($O_2$ concentration <0.1 ppm) maintained at 10 °C using ammonium bicarbonate buffer at pH 9.1. Under these conditions, no decomposition was observed at least for 3 h (Figure 3a).

MoaA reaction conditions were chosen to maximize the production of 3′,8-cH$_2$GTP, as well as the percentage conversion of GTP to 3′,8-cH$_2$GTP. It was important to consume as much GTP as possible in the MoaA reaction because of the close separation between GTP and 3′,8-cH$_2$GTP during purification with anion-exchange resin. The reaction is limited by the substoichiometric turnover of MoaA. The maximum turnover observed after 60 min of incubation at 25 °C was 0.5 ± 0.2 when stoichiometric or excess amount of GTP relative to MoaA was used (Figure 2c). The use of substoichiometric amount of GTP to MoaA significantly lowered the yield. Thus, for the isolation of 3′,8-cH$_2$GTP, GTP concentration was kept stoichiometric relative to MoaA.

Purification conditions also required careful optimization to avoid decomposition. Successful purification was achieved by the use of two anion-exchange columns. A strong anion-exchange resin (QAE Sepharose) was used as the first step of purification to process a large volume of sample and to separate 3′,8-cH$_2$GTP and GTP from the other components in the MoaA assay mixture. A weak anion-exchange resin (DEAE Sepharose) was used to separate GTP from 3′,8-cH$_2$GTP (see Figure S3 for the chromatograms). Typically, 10 $\mu$mol of 3′,8-cH$_2$GTP was isolated from 200 mL of enzyme reaction mixture containing 0.2 mM MoaA, 0.2 mM GTP, 1.0 mM SAM, and 1.0 mM sodium dithionite. The isolated 3′,8-cH$_2$GTP had a unique absorption feature at 322 nm ($\varepsilon_{322nm}$ = 5.1 ± 1.1 mM$^{-1}$ cm$^{-1}$, Figure 3b, bold trace). This absorption feature also exhibited oxygen sensitivity and diminished upon exposure to air (Figure 3b, thin traces), consistent with the oxygen sensitivity of 3′,8-cH$_2$GTP observed by the biochemical characterization (Figure 3a).

The isolated 3′,8-cH$_2$GTP was also analyzed for the number of phosphates in the molecule, as its close migration with GTP on the anion-exchange resin suggested the presence of a triphosphate group. The use of a colorimetric phosphate assay[39] after a phosphatase treatment revealed 2.93 ± 0.03


dx.doi.org/10.1021/ja401781t | J. Am. Chem. Soc. 2013, 135, 7019−7032

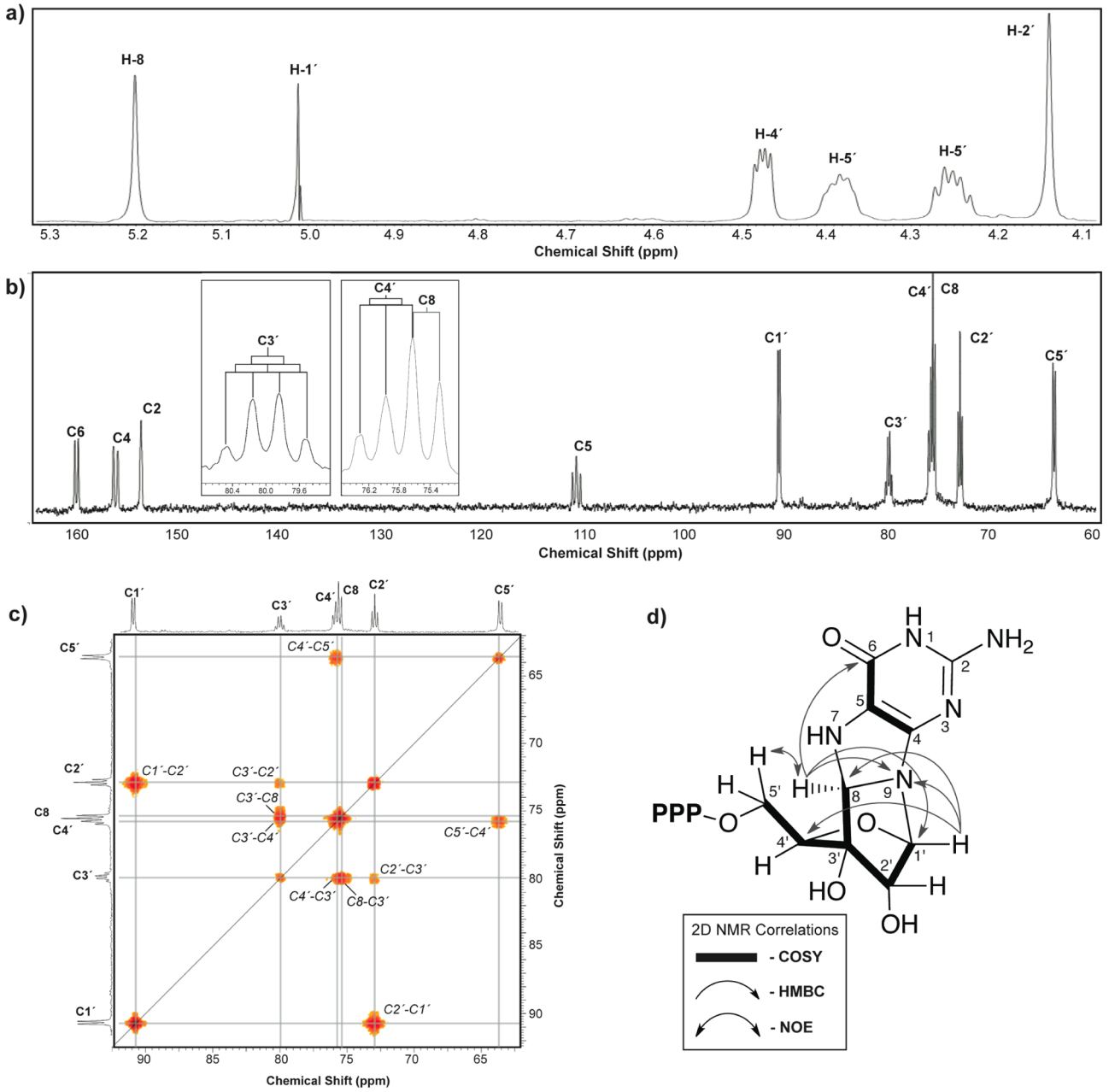


**Figure 4.** NMR structural characterization of 3′,8-cH$_2$GTP. (a) $^1$H NMR (600 MHz, D$_2$O) and (b) $^1$H-decoupled $^{13}$C NMR (200 MHz, D$_2$O) spectra of 3′,8-cH$_2$GTP and [U-$^{13}$C$_{10}$, $^{15}$N$_5$]3′,8-cH$_2$GTP, respectively. No signal associated with 3′,8-cH$_2$GTP was observed outside the shown chemical shift range. The intensity of the H-1′ signal in (a) was decreased due to the water suppression at 4.95 ppm. The insets in (b) shows magnified view of the signals for C-3′, C-4′ and C-8. (c) $^{13}$C−$^{13}$C COSY spectrum of [U-$^{13}$C$_{10}$,$^{15}$N$_5$]3′,8-cH$_2$GTP. The assignments for the observed correlations are indicated. The chemical shift region for C-1′ through C-5′ and C-8 is shown. The spectrum with full chemical shift range is available in Figure S6. (d) $^{13}$C−$^{13}$C COSY (bold), and selected $^1$H−$^{13}$C, and $^1$H−$^{15}$N HMBC (single-headed arrows) correlations, and NOE (a double-headed arrow). A complete list of the observed HMBC correlations is available in Table 1. **P** designates a phosphate group.

phosphate groups per molecule. This result is consistent with 3′,8-cH$_2$GTP being a triphosphate compound.

**Molecular Weight Determination of 3′,8-cH$_2$GTP.** An ESI-TOF-MS analysis of isolated 3′,8-cH$_2$GTP revealed $m/z$ = 521.984 ± 0.001 [M−H]$^-$ (Figure S4a), consistent with the molecular formula of $C_{10}H_{15}N_5O_{14}P_3$ (calcd $m/z$ = 521.983 [M−H]$^-$). The observed mass was also consistent with GTP, which migrates close to 3′,8-cH$_2$GTP during the anion-exchange chromatographies (see Figure S3), and occasionally contaminated 3′,8-cH$_2$GTP. Thus, it was important to verify that the observed signal was indeed associated with 3′,8-cH$_2$GTP rather than contaminating GTP. To distinguish 3′,8-cH$_2$GTP from GTP, purified 3′,8-cH$_2$GTP was incubated with MoaC and analyzed by MS, which exhibited no MS signal at $m/z$ = 521.984, and instead exhibited a signal at $m/z$ = 362.052 ± 0.001 [M−H]$^-$ (Figure S4b) corresponding to a hydrate form of cPMP ($m/z$ [M−H]$^-$ calcd for $C_{10}H_{13}N_5O_8P$, 362.051). These findings suggest that the observed MS signal was indeed associated with the intact 3′,8-cH$_2$GTP, but not contaminating GTP.

**Structural Characterization of 3′,8-cH$_2$GTP by NMR Spectroscopy.** Further structural characterization of 3′,8-


dx.doi.org/10.1021/ja401781t | J. Am. Chem. Soc. 2013, 135, 7019−7032

**Table 1. Summary of NMR Data for 3′,8-cH$_2$GTP**

| | NMR | | COSY | | HMBC | | |
|---|---|---|---|---|---|---|---|
| no. | $^{13}$C, $\delta$ (ppm) (m, $J_{CC}$(Hz)) | $^{1}$H $\delta$ (ppm) (m, $J_{HH}$(Hz)) | $^{1}$H−$^{1}$H | $^{13}$C−$^{13}$C | $^{1}$H−$^{13}$C | $^{1}$H−$^{15}$N | NOESY |
| 2 | 153.6 (s) | | | | | | |
| 4 | 156.1 (d, 83.1) | | | C-5 | | | |
| 5 | 110.8 (t, 76.0) | | | C-4, C-6 | | | |
| 6 | 160.0 (d, 68.0) | | | C-5 | H-8 | | |
| 8 | 75.6 (d, 42.5) | 5.20 (s) | | C-3′ | H-1′, H-4′ | N-9 | H-5′a |
| 1′ | 90.8 (d, 40.0) | 5.02 (s) | | C-2′ | H-2′, H-8 | N-9 | |
| 2′ | 73.0 (t, 40.0) | 4.14 (s) | | C-1′, C-3′ | H-8 | | |
| 3′ | 80.0 (q, 39.9) | | | C-8, C-2′, C-4′ | H-1′, H-2′, H-4′ | | |
| 4′ | 75.9 (t, 42.0) | 4.48 (dd, 3.9, 7.3) | H-5′a, H-5′b | C-3′, C-5′ | H-8, H-1′, H-2′, H-5′ | | |
| 5′a | 63.7 (d, 44.9) | 4.25 (dt,[a] 11.3, 6.2) | H-4′, H-5′b | C-4′ | | | H-8 |
| 5′b | | 4.39 (dt,[a] 11.3, 5.3) | H-4′, H-5′a | | | | |

[a]The doublet feature is derived from a $^{2}J_{^{1}H-^{1}H}$ to the geminal $^{1}$H, and the triplet feature is from a $^{3}J_{^{1}H-^{1}H}$ to H-4′ and a $^{3}J_{^{31}P-^{1}H}$ to $^{31}$P of the phosphate group.

cH$_2$GTP was carried out using NMR spectroscopy. Figure 4a shows the $^{1}$H NMR spectrum of purified 3′,8-cH$_2$GTP with six signals between 4.1 and 5.3 ppm. To confirm that these signals are associated with 3′,8-cH$_2$GTP, the observed $^{1}$H NMR signals were quantified by comparing the integrals of the observed signals with that of a known concentration of maleic acid as an internal standard. The concentration of 0.59 ± 0.14 mM was determined by this analysis, which agreed well with the concentration (0.67 ± 0.03 mM) biochemically determined after its conversion to compound Z.

The $^{13}$C NMR spectrum (Figure 4b) was recorded on 3′,8-cH$_2$GTP uniformly labeled with $^{13}$C and $^{15}$N, prepared from [U-$^{13}$C$_{10}$,$^{15}$N$_5$]GTP. Four carbon signals were found at 111, 154, 156, and 160 ppm, suggesting the presence of four sp$^2$ carbons. The major multiplicities of the $^{13}$C NMR signals (Figure 4b) are derived from $^{1}J_{^{13}C-^{13}C}$ coupling. The analysis of the multiplicities (Figure 4b and Table 1) in combination with the $^{13}$C−$^{13}$C COSY correlations (Figure S6; all 2D NMR spectra are available in the Supporting Information) established the connectivities among the signals at 111, 156, and 160 ppm. Together with the comparison with the chemical shifts reported for various purines and pyrimidines (Table S1),[44,45] we assigned the four sp$^2$ carbon signals to the carbons in the 6-hydroxy-2,4,5-triaminopyrimidine moiety of 3′,8-cH$_2$GTP.

The remaining $^{13}$C NMR signals were found between 63.7 and 90.8 ppm with observed $^{1}J_{^{13}C-^{13}C}$ coupling constants of ∼40 Hz (Figure 4b and Table 1), suggesting that they are all sp$^3$ carbons.[46] The analysis of the multiplicities in combination with the $^{13}$C−$^{13}$C COSY correlations (Figure 4c) unambiguously determined the C−C connectivities as shown in Figure 4d. The most notable is the presence of C-3′ as a tertiary carbon that appeared as a quartet signal in the $^{13}$C NMR spectrum (see the inset of Figure 4b). The connectivity of C-3′ to C-8 in addition to C-2′ and C-4′ was established by the $^{13}$C−$^{13}$C COSY correlations (Figure 4c,d). This feature distinguishes this molecule from GTP, cPMP, or molecules that have been previously proposed as MoaA products, 2-amino-5-formylamino-6-ribofuranosylamino-4-pyrimidinone triphosphate (**6**), and pyranopterin triphosphate (**7**),[29,30] because none of these molecules has a tertiary carbon. This analysis suggested that during the MoaA reaction, the C3′−C8 bond is formed, but the pyranopterin structure is not yet established.

Further NMR analysis provided a basis for the complex multi-ring structure around C-8. $^{1}$H−$^{13}$C HMQC (Figure S7), multiplicity of the $^{13}$C NMR signal (Figure 4b), and the $^{13}$C−$^{13}$C COSY correlation (Figure 4c) suggested that C-8 is a methine primary carbon. The $^{1}$H−$^{13}$C HMBC correlations from H-8 to C-1′, and from H-1′ to C-8 (Figure 4d), suggested a connection between C-8 and C-1′ through a heteroatom. The $^{1}$H−$^{15}$N HMBC correlations to the same N from H-1′ and from H-8 (Figure 4d) suggested that the bridging heteroatom is N. The second heteroatom on C-8 would be either N or O. The reported chemical shift values for methine primary carbons covalently bound to an N and an O are 84−97 ppm,[31,47−49] whereas those with two N's are 71−86 ppm.[48,50−53] Thus, the chemical shift observed for C-8 (75.6 ppm) is most consistent with the presence of the second N on C-8.

The connections of C-1′ and C-8 to nitrogen atoms suggested the connections to 6-hydroxy-2,4,5-triaminopyrimidine because all nitrogen atoms are associated with the 6-hydroxy-2,4,5-triaminopyrimidine based on the molecular formula determined by MS. The connection to 6-hydroxy-2,4,5-triaminopyrimidine is supported by the observation of a weak $^{1}$H−$^{13}$C HMBC correlation from H-8 to C-6 (Figures 4d and S9). While several different orientations for 6-hydroxy-2,4,5-triaminopyrimidine are consistent with the NMR data (see Figure S11 for possible structures), the nitrogen bridging C-8 and C-1′ is likely N-9, considering that the previous isotope tracer experiments indicated that the N9−C1′ bond is maintained during the transformation of GTP into cPMP.[7,17] The second N on C-8 was assigned as N-7, considering that C8−N7 bond is present in GTP, and there is no evidence suggesting that the other Ns are involved in the transformation of GTP to cPMP. On the basis of these analyses, we propose the orientation of the 6-hydroxy-2,4,5-triaminopyrimidine connection as shown in Figure 4d.

The structures of the remaining part of the molecule were based on the following analysis. The furanose ring was based on the $^{1}$H−$^{13}$C HMBC correlations from H-1′ to C-4′ (Figure 4d). The position of the triphosphate group was based on the $^{3}J_{HP}$ = 5−6 Hz observed for the $^{1}$H NMR signals for H-5′a and H-5′b (Figure 4a and Table 1), which are comparable to those reported for various nucleotides.[54,55] The hydroxyl groups at the 2′ and 3′ positions were based on the NMR chemical shifts observed for H-2′, C-2′, and C-3′. The stereochemistry at C-1′, C-2′, C-3′, and C-4′ is based on GTP and cPMP.[56] The absence of an apparent $J$ coupling between H-1′ and H-2′ ($^{3}J_{H1'H2'}$ < 4 Hz) is consistent, based on the Karplus relations,[57]


dx.doi.org/10.1021/ja401781t | J. Am. Chem. Soc. 2013, 135, 7019−7032

**Table 2. Steady-State Kinetic Parameters for MoaA, MoaC, and MOCS1B**

| enzyme | substrate | $K_m$ ($\mu$M) | $k_{cat}$ ($min^{-1}$) | $k_{cat}/K_m$ ($\mu M^{-1}$ $min^{-1}$) |
|---|---|---|---|---|
| MoaA | GTP | 1.4 ± 0.2 | 0.045 ± 0.003 | 0.032 ± 0.012 |
| | SAM | 4.1 ± 1.3 | 0.043 ± 0.004 | 0.011 ± 0.003 |
| MoaC | 3′,8-cH$_2$GTP | <0.060 | 0.17 ± 0.026 | >2.8 |
| MOCS1B[a] | 3′,8-cH$_2$GTP | 0.79 ± 0.24 | 0.092 ± 0.020 | 0.12 ± 0.08 |

[a]Purified MOCS1B was a complex of a full-length peptide (26 kDa) with two N-terminally truncated peptides (18 and 16 kDa). See Figure S14 for details.

with the calculated dihedral angle of 59° between H1′−C1′−C2′−H2′ (see Figure S12 for the energy-minimized conformation of 3′,8-cH$_2$GTP). The stereochemistry at C-8 is based on NOE observed between H-8 and H-5′a (Figure 4d, a double-headed arrow).

On the basis of all the analyses described above, we propose the structure of the isolated molecule as (8*S*)-3′,8-cyclo-7,8-dihydroguanosine 5′-triphosphate (3′,8-cH$_2$GTP, Figure 4d). The proposed structure is consistent with all the NMR data (Table 1), as well as MS, phosphate assay, and chemical derivatization to DMPT described above.

**Relevance of 3′,8-cH$_2$GTP to Moco Biosynthesis.** The physiological relevance of 3′,8-cH$_2$GTP as an intermediate of Moco biosynthesis was further investigated by steady-state kinetics of the MoaA- and MoaC-catalyzed reactions. The kinetic parameters for the MoaC-catalyzed conversion of 3′,8-cH$_2$GTP to cPMP were determined using purified 3′,8-cH$_2$GTP as the substrate. The kinetic parameters for the MoaA-catalyzed reaction were determined by a coupled assay in the presence of a 10-fold excess of MoaC to ensure efficient conversion of 3′,8-cH$_2$GTP to cPMP. In both assays, cPMP was converted to compound Z and quantified by HPLC. The results are summarized in Table 2. The $k_{cat}$ of MoaC was ∼4-fold greater than that of MoaA determined by this method, and the $K_m$ of MoaC for 3′,8-cH$_2$GTP was <0.06 $\mu$M, the lower limit of detection. $K_m$ of MoaA for GTP was found to be 1.4 ± 0.2 $\mu$M, which may be compared to the previously reported binding constant of 0.29 ± 0.11 $\mu$M determined by an equilibrium dialysis.[26] These observations support the conclusion that 3′,8-cH$_2$GTP is likely the physiological substrate of MoaC, and the biosynthetic intermediate between GTP and cPMP during Moco biosynthesis.

The relevance of 3′,8-cH$_2$GTP as an intermediate in human Moco biosynthesis was investigated by the characterization of a human homologue of MoaC. Previous gene complementation studies suggested that the human proteins, MOCS1A and MOCS1B, have functions that correspond to those of MoaA and MoaC, respectively.[37] In human cells, MOCS1B is expressed as an N-terminal fusion with a catalytically inactive MOCS1A.[20,37] Since we have not been successful in obtaining the fusion protein, the stand-alone MOCS1B domain was expressed as an N-terminal His-tag protein, and purified by Ni-affinity chromatography. SDS-PAGE and MS analysis of the purified protein revealed that MOCS1B (26 kDa) was co-purified with two other shorter MOCS1B peptides (16 and 18 kDa) truncated at the N-terminus (see Figure S14 for details of characterization). The ratio of the truncated MOCS1B to the full length MOCS1B was not altered by the use of protease inhibitor cocktails or further purification by anion-exchange, size exclusion, and phenyl sepharose column chromatography. Because the truncation occurred only in the poorly conserved N-terminal region of MOCS1B (see Figure S14c for a multiple sequence alignment), we used this MOCS1B for further characterization. The HPLC analysis of the product of the MOCS1B activity assay with 3′,8-cH$_2$GTP as the substrate revealed that cPMP was formed with the kinetic parameters of $K_m$ = 0.79 ± 0.24 $\mu$M and $k_{cat}$ = 0.092 ± 0.020 $min^{-1}$, which are somewhat less efficient than but comparable to $K_m$ and $k_{cat}$ determined for MoaC (Table 2). While these kinetic parameters could be affected by the observed truncation at the N-terminus and/or the lack of the MOCS1A domain, the results show that 3′,8-cH$_2$GTP is a substrate for MOCS1B, and thus suggest that 3′,8-cH$_2$GTP may be a biosynthetic intermediate in human Moco biosynthesis as well.

**Stoichiometry of the MoaA Reaction and the Position of H-Atom Abstraction.** Since MoaA is a member of the radical SAM superfamily, the conversion of GTP to 3′,8-cH$_2$GTP is likely initiated by a radical formation at C-3′ by 5′-dA$^{\bullet}$ formed by reductive cleavage of SAM, followed by the attack of C-3′ to C-8. In the reactions catalyzed by radical SAM enzymes, SAM may be consumed as a co-substrate, or regenerated and used as a co-catalyst.[23] Since the conversion of GTP into 3′,8-cH$_2$GTP could take place either of the two mechanisms, we quantified the amount of 5′-dA and cPMP formed in the MoaA/MoaC coupled assay. A 2-fold excess of MoaC was used relative to MoaA to ensure complete conversion of 3′,8-cH$_2$GTP to cPMP. HPLC quantitation of 5′-dA suggested that, under this condition, stoichiometric amounts of 5′-dA and 3′,8-cH$_2$GTP were formed (Figure 5a).

The determination of the stoichiometry of SAM cleavage for radical SAM enzymes has been frequently obscured by abortive production of 5′-dA.[58] While our data are consistent with stoichiometric formation of 5′-dA, it is important to show that the observed 5′-dA is indeed the product of H-atom abstraction from GTP, but not a product of abortive SAM cleavage. Thus, we investigated the transfer of a deuterium atom on GTP into 5′-dA. Based on the structure of 3′,8-cH$_2$GTP, the reaction most likely proceeds through H-abstraction from the 3′ position. Thus, [3′-$^2$H]GTP was chemoenzymatically prepared from [3-$^2$H]ribose, and used to investigate a deuterium transfer from [3′-$^2$H]GTP to 5′-dA. When [3′-$^2$H]GTP was used as a substrate, a small but significant kinetic isotope effect of $V_H/V_D$ = 1.28 ± 0.05 was observed (Figure 5b), which is comparable to a value previously reported for another radical SAM enzyme, BtrN ($V_H/V_D$ = 1.3 ± 0.1).[59]

To investigate the H-3′ transfer from GTP to 5′-dA, 5′-dA was isolated from a large scale MoaA/MoaC coupled reaction mixture, where [3′-$^2$H]GTP (98 $\mu$M) was incubated with MoaA (50 $\mu$M), MoaC (100 $\mu$M), SAM (1 mM), and sodium dithionite (1 mM) at 25 °C for 60 min. HPLC analysis of this assay solution revealed formation of 48 ± 2 $\mu$M of 5′-dA and 47 ± 2 $\mu$M of cPMP. 5′-dA was isolated using reverse-phase silica gel column chromatography and HPLC, and characterized by MS (Figure 5c), and $^1$H and $^2$H NMR spectroscopies (Figure 5d). These analysis revealed incorporation of a single deuterium atom in the 5′-methyl group of 5′-dA, consistent

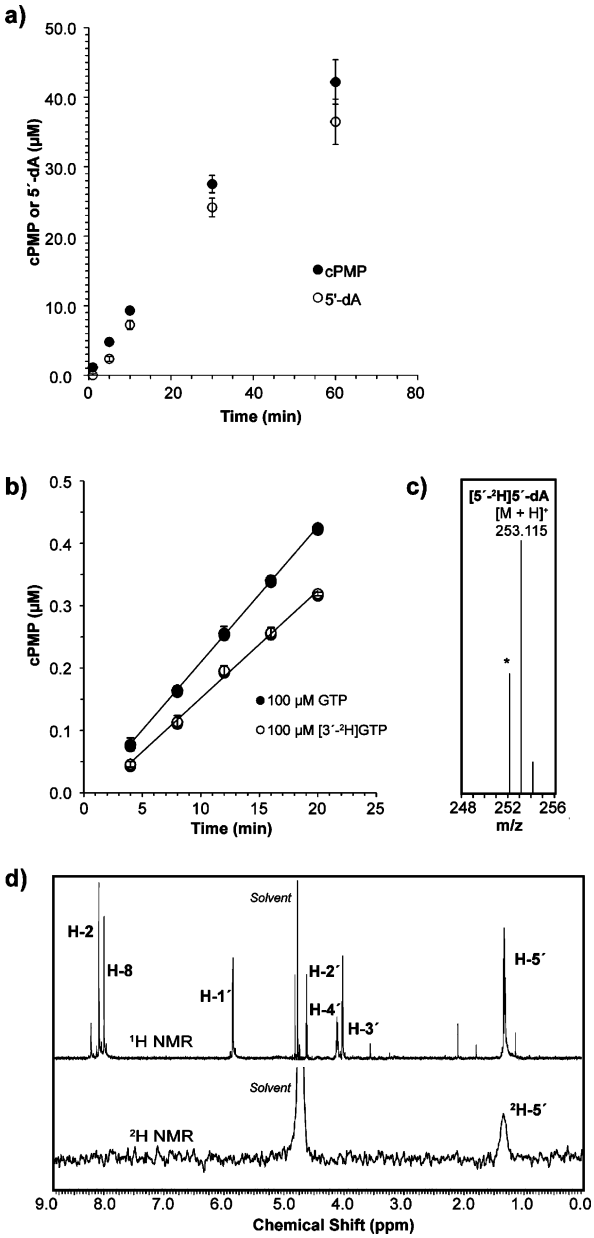


**Figure 5.** Mechanistic studies on the MoaA-catalyzed H-atom abstraction. (a) Stoichiometry of formation of 5′-dA (open circles) and cPMP (filled circles) in the MoaA/MoaC coupled assay. MoaA (20 $\mu$M) was incubated with GTP (1 mM), SAM (1 mM) and sodium dithionite (1 mM) in the presence of MoaC (40 $\mu$M) at 25 °C. cPMP was quantified by HPLC after its conversion to compound Z. Each point is an average of 3−6 replicates, and the error bars are calculated on the basis of the standard deviation. (b) Rate of cPMP formation from GTP or [3′-$^2$H]GTP by MoaA and MoaC. MoaA (0.5 $\mu$M) was incubated with GTP or [3′-$^2$H]GTP (0.1 mM) in the presence of sodium dithionite (1 mM), SAM (1 mM) and MoaC (5 $\mu$M) at 25 °C. cPMP was quantified by HPLC after its conversion to compound Z. Each point is an average of four replicates, and the error bars are calculated on the basis of the standard deviation. (c) ESI-TOF-MS and (d) $^1$H NMR (600 MHz in $D_2O$) and $^2$H NMR (76.75 MHz in $H_2O$) spectra of 5′-dA isolated from the reaction in the presence of MoaA (50 $\mu$M), MoaC (100 $\mu$M), SAM (1 mM), [3′-$^2$H]GTP (98 $\mu$M, 94 ± 3% atom $^2$H), and sodium dithionite (1 mM). The signal indicated with * is non-deuterated 5′-dA ($m/z$ [M+H]$^+$ calcd for $C_{10}H_{14}N_5O_3$ 252.110, found 252.111), presumably derived from non-labeled GTP (see main text).

with a recent observation by Mehta et al.[30] Under the conditions we investigated, ∼30% of 5′-dA was formed with no deuterium incorporation (Figure 5c). We attribute this mainly to the incomplete labeling of [3′-$^2$H]GTP (94 ± 3 atom % $^2$H) and the presence of non-labeled GTP copurified with MoaA. The amount of co-purified GTP was determined as 16 ± 1% that of MoaA by HPLC after its release from MoaA by acid denaturing. Together with the ∼50% conversion of [3′-$^2$H]GTP to cPMP, these observations suggest that majority of the non-labeled 5′-dA formed in this reaction was originated from the non-labeled GTP in the sample. Thus, our observation is consistent with a mechanism in which MoaA catalyzes H-abstraction from the 3′ position of GTP by stoichiometric consumption of SAM.

## ■ DISCUSSION

This report describes the isolation and structural characterization of 3′,8-cH$_2$GTP, a missing intermediate in Moco biosynthesis. Our stepwise assay indicated that there is a small molecule that is produced by MoaA in the presence of GTP, SAM, and dithionite, and that may serve as a substrate of MoaC. This compound was isolated from the *in vitro* MoaA assay mixture using two sequential anion-exchange column chromatographies under strict anaerobic conditions, and structurally characterized by chemical derivatization, MS and NMR spectroscopy. The physiological relevance of the isolated 3′,8-cH$_2$GTP was investigated by the steady-state kinetic analysis of MoaC or its human homologue, MOCS1B. In these analyses, both enzymes catalyze the conversion of 3′,8-cH$_2$GTP to cPMP with high specificities ($K_m$ values of <0.060 and 0.79 $\mu$M, respectively). Although the observed turnover rates for MoaA ($k_{cat}$ = 0.053 min$^{-1}$) and MoaC ($k_{cat}$ = 0.17 min$^{-1}$) were slow, they are typical for enzymes in cofactor biosynthesis,[60,61] including other steps of Moco biosynthesis,[62] which may be attributed to the small amount of cofactors required in the cells. Thus, our data presented here suggest that 3′,8-cH$_2$GTP may represent the physiologically relevant intermediate of Moco biosynthesis.

The MoaA reaction product has been described previously. Schindelin and Hänzelmann[26] first stated in their publication that in the reaction of MoaA with SAM and GTP without MoaC they observed the formation of small molecule that may be converted to DMPT. Unfortunately, no data were presented. Our analysis in this report provides strong evidence that MoaA product indeed has an acid-labile 6-hydroxy-2,4,5-triaminopyrimidine moiety that may be converted to DMPT. More recently, Mehta et al. reported the observation of a molecule with a light absorption feature at 320 nm in the LCMS analysis of the reaction mixture of MoaA incubated with GTP, SAM, and dithionite. The observation of a mass signal at $m/z$ = 524 [M+H]$^+$ at the same retention time led the authors to propose this molecule as pyranopterin triphosphate (7, Figure 1c). While this conclusion is distinct from ours, the reported light absorption feature and the mass signal are also consistent with 3′,8-cH$_2$GTP. In addition, Mehta et al. mentioned that the observed molecule was oxygen sensitive, which is also a characteristic of 3′,8-cH$_2$GTP. On the other hand, our NMR data are inconsistent with pyranopterin triphosphate. Thus, we conclude that the previously described putative MoaA products[26,30] were indeed 3′,8-cH$_2$GTP.

It is noteworthy that Mehta et al. also considered 3′,8-cH$_2$GTP as an intermediate of cPMP biosynthesis, but suggested to exist only transiently during the MoaA-catalyzed


dx.doi.org/10.1021/ja401781t | J. Am. Chem. Soc. 2013, 135, 7019−7032

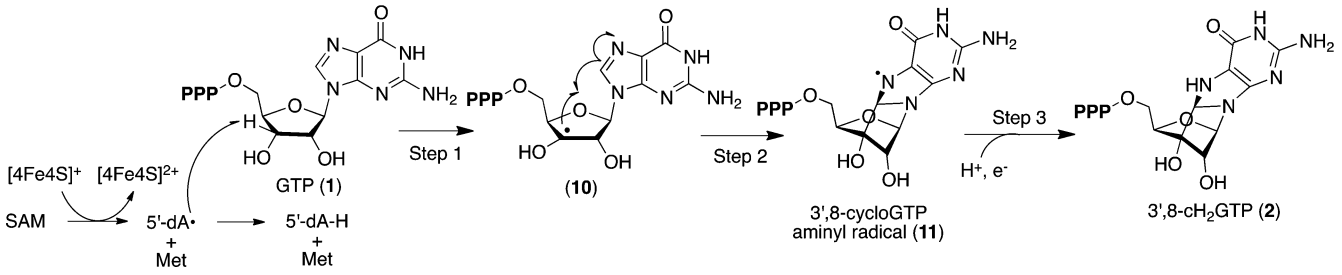


**Figure 6.** Proposed mechanism for the MoaA-catalyzed conversion of GTP to 3′,8-cH$_2$GTP.

conversion of GTP to pyranopterin triphosphate.[30] This proposal appears to be based mostly on their observation of the deuterium transfer from the 3′ position of GTP to 5′-dA, and their proposal for pyranopterin triphosphate as a MoaA product, which we now believe to be a mis-assignment. While their deuterium tracer experiments support the formation of a radical at C-3′, prior to our work, to our knowledge, there was no precedent for the reaction between a C-3′ centered radical and C-8 in purine nucleosides or nucleotides. In addition, the radical formation at C-3′ could also be consistent with the previous proposals with **6** as an intermediate (Figure 1b)[29,33] if the H-3′ abstraction was to take place after the formation of **6**. There are precedents for formyl group transfer reactions by radical mechanisms.[63] Our isolation and characterization of 3′,8-cH$_2$GTP as a MoaA product provides strong evidence for the function of MoaA to catalyze the conversion of GTP to 3′,8-cH$_2$GTP. As 3′,8-cH$_2$GTP can be chemically derivatized to DMPT, our model is also consistent with the observations by Schindelin and Hänzelmann.[26]

Our identification of 3′,8-cH$_2$GTP as the product of MoaA as well as the substrate of MoaC is a sharp contrast to the previous consensus in the field, where MoaA was considered largely responsible for the formation of the pyranopterin ring, and a relatively minor role was considered for MoaC.[29,30] Our observations suggest that MoaC plays a major role in the formation of pyranopterin ring. The reactions catalyzed by MoaA and MoaC may be compared to the conversion of GTP into 7,8-dihydroneopterin triphosphate by GTP cyclohydrolase I in folate biosynthesis (see Figure S1a). The first step of the GTP cyclohydrolases I reaction is the hydrolysis of the imidazole moiety of the guanine base using a water activated on $Zn^{2+}$ in the active site.[31,64] This hydrolysis triggers the ensuing complex Amadori rearrangement[18,65−67] that takes place in the same active site.[68,69] Our results suggest that Moco biosynthesis is also initiated by modification of GTP at the C-8 position, but to a distinct molecule, 3′,8-cH$_2$GTP. In contrast to GTP cyclohydrolases I, MoaA is incapable of catalyzing the rearrangement reactions, presumably due to the lack of appropriate amino acid residues in the active-site. Instead, 3′,8-cH$_2$GTP is transferred to MoaC where a complex rearrangement reaction proceeds. In the following paragraphs, we will discuss the mechanisms of the reactions catalyzed by each of these two enzymes.

The observation of 3′,8-cH$_2$GTP formed from GTP by a radical SAM enzyme, MoaA, indicated to us that the reaction would proceed through a H-atom abstraction from the 3′ position. This is consistent with the deuterium tracer experiments by Mehta et al.[30] In reactions catalyzed by radical SAM enzymes, SAM may be used catalytically or stoichiometrically. However, the demonstration of the stoichiometry for radical SAM-catalyzed reactions is frequently complicated by abortive cleavage of SAM, where SAM is reductively cleaved to methionine and 5′-dA regardless of product formation. The abortive SAM cleavage has been reported for many radical SAM enzymes to various degrees.[58,70−74] A notable example is the recent report on QueE by McCarty et al.[70] QueE catalyzes a complex rearrangement of 7-carboxy-7-deazaguanine to 6-carboxy-5,6,7,8-tetrahydropterin during deazapurine biosynthesis. Although SAM is used catalytically in this reaction, detectable amount of 5′-dA was formed and contained deuterium atoms that originated from substrate. Thus, although previous studies indicated a transfer of a deuterium atom at the 3′ position of GTP to 5′-dA,[30] the lack of knowledge about the stoichiometry of the reaction left significant ambiguity about how SAM is used in the MoaA reaction. Our observation of the stoichiometric formation of 5′-dA and cPMP in the MoaA/MoaC coupled assay, in combination with the demonstration of the stoichiometric transfer of a deuterium atom at the 3′ position of GTP to the methyl group of 5′-dA, is consistent with the stoichiometric consumption of SAM and H-atom abstraction from the 3′ position.

On the basis of the observations described above and our structural characterization of 3′,8-cH$_2$GTP, in combination with chemical precedents and the reported structures of MoaA, we propose a mechanism for the MoaA-catalyzed reaction (Figure 6). Our deuterium tracer experiments and those reported by Mehta et al.[30] suggested that the reaction is initiated by the abstraction of H-3′ by 5′-dA$^{\bullet}$, generated by the reductive cleavage of SAM using the N-terminal 4Fe-4S cluster as a reductant. The resulting C-3′ radical (**10**) then attacks C-8 and generates a 3′,8-cycloGTP aminyl radical intermediate **11**, which is then converted to 3′,8-cH$_2$GTP. While the aminyl radical **11** could be reduced by a re-abstraction of H-atom from 5′-dA, our observation of the stoichiometric formation of 5′-dA in the MoaA/MoaC coupled assay relative to cPMP disfavors such mechanism. Thus, another electron source is required. One possible reductant is the C-terminal [4Fe-4S] cluster that binds GTP.[26,27] A reduction of 5′,8-cyclo-deoxyadenosine aminyl radical by reduced methylviologen ($E°$ = −0.45 V)[75] has been reported. Thus, considering the reported redox potentials of related [4Fe-4S] clusters ($E°$ = −0.4 to −0.6 V),[76,77] the C-terminal [4Fe-4S] cluster may carry out the reduction of the aminyl radical. The redox role of the C-terminal [4Fe-4S] cluster may be probed by EPR spectroscopy[36] and is currently being investigated in our laboratory.

The reduction of the aminyl radical **11** may also be facilitated by the three conserved Arg residues, R17, R266, and R268 (numbering based on *S. aureus* MoaA), which are 3.2−4.6 Å from N-7 of GTP in the crystal structure.[26] Mutations in these residues have been found in Moco-deficient patients.[78] MoaA variants with mutations in these residues still bind GTP to a various degree, but do not produce cPMP when assayed with


dx.doi.org/10.1021/ja401781t | J. Am. Chem. Soc. 2013, 135, 7019−7032

MoaC.[26] These Arg residues may be assisting the aminyl radical reduction by electrostatic stabilization of the anionic charge on the base, or by providing a $H^+$. Controlled movements of protons and electrons are often critical for redox reactions in enzyme catalysis.[79]

Another important feature of the active-site of MoaA is the presence of conserved hydrophobic amino acid residues, V167, I194, and I253, surrounding 2′-OH and 3′-OH of GTP (Figure 7).[26] No amino acid residues are in H-bonding interaction

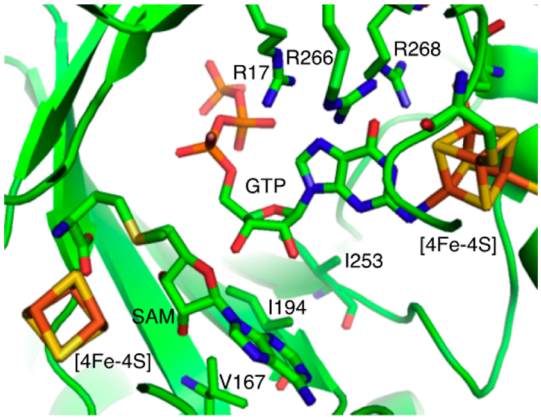


**Figure 7.** Model of the MoaA active site. SAM was modeled into the X-ray crystal structure of MoaA in complex with GTP[26] (PDB ID: 2FB3) based on the structural alignment with the X-ray crystal structure of MoaA in complex with SAM[9] (PDB ID: 1TV8). Oxygens are shown in red, nitrogens in blue, sulfurs in yellow, phosphorus in orange, and irons in brown.

distance from 2′-OH and 3′-OH, which is inconsistent with the earlier proposal where MoaA catalyzes complex rearrangement reactions that require general acid/base catalysis at 3′-OH.[30] On the other hand, the structural feature of MoaA active site is consistent with our proposal for the function of MoaA to catalyze the conversion of GTP to 3′,8-$cH_2$GTP, in which no general acid/base catalysis is required.

The hydrophobic environment around 2′-OH and 3′-OH of GTP may also be important for directing the reaction of C-3′ centered radical with C-8 by preventing side reactions. To our knowledge, the reaction of C-3′ radical with C-8 of purine nucleoside/nucleotide is unprecedented.[28,42,80] Radical formation at C-3′ in DNA and RNA results in a formation of 3′-keto-2′-deoxyribonucleotides or a C3′−C4′ bond cleavage by complex mechanisms.[80] Reactions of the C-3′ nucleotide radical in enzymes have been extensively studied for ribonucleotide reductase (RNR),[81,82] where the radical formation on C-3′ facilitates dissociation of 2′-OH. Mechanistic studies on RNR and related synthetic model systems suggest that the dissociation of 2′-OH requires general acid/base catalysts at 2′-OH and 3′-OH.[82] The difference in the active-site structures of MoaA and RNR that both generate a radical at C-3′, but produce distinct products, may indicate the mechanism by which enzymes control radical reactions. The roles of the MoaA active site amino acid residues are currently under investigation.

The following complex rearrangement reactions are catalyzed by MoaC. While MoaC was previously known to be essential for the biosynthesis of cPMP,[7,9,20,21] the lack of understanding about the structure of the substrate of MoaC precluded identification of the exact role of this enzyme during the conversion of GTP into cPMP. Thus, our finding that 3′,8-$cH_2$GTP may be the physiological substrate provides a means to study the mechanism of the complex rearrangement reaction catalyzed by MoaC.

The structures of MoaC[32−35,83] or previous in vitro characterization of MoaC in the presence of MoaA[9] did not reveal any complex cofactor or metals in MoaC. Thus, the MoaC reaction appears to take place via general acid/base catalysis using amino acid side chain of MoaC. Our characterization of 3′,8-$cH_2$GTP suggested susceptibility of this molecule to acid hydrolysis. Thus, the transformation of GTP into 3′,8-$cH_2$GTP by MoaA may be sufficient to make this molecule susceptible to complex rearrangement by MoaC presumably using general acid/base catalysts. While several different mechanisms may be possible, Figure 8 shows a

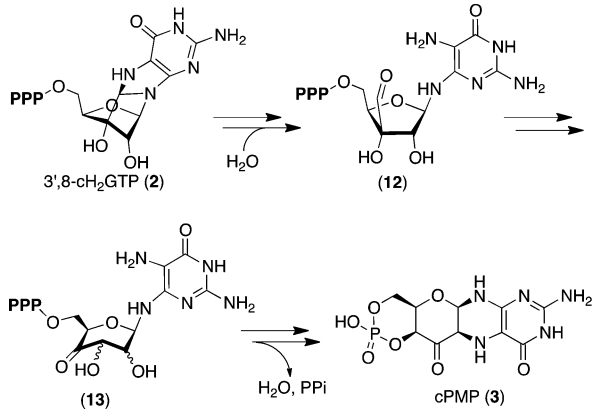


**Figure 8.** Possible mechanism of the MoaC-catalyzed conversion of 3′,8-$cH_2$GTP to cPMP. **P** designates a phosphate group.

possible mechanism for the conversion of 3′,8-$cH_2$GTP to cPMP by MoaC most consistent with the currently available chemical and enzymological precedents. The reaction is likely initiated by hydrolysis of the constrained pyrrolidine and imidazoline rings of 3′,8-$cH_2$GTP to an aldehyde **12**, based on the susceptibility of 3′,8-$cH_2$GTP to acid hydrolysis during derivatization to DMPT (Figure 2b). Acid hydrolysis of various aminal molecules has been well documented.[84] The aldehyde **12** is then converted to a hexose **13**. The mechanism of this reaction could be either a retroaldol−aldol rearrangement initiated by the deprotonation at 2′-OH, or an $\alpha$-ketol rearrangement initiated by the deprotonation at 3′-OH. A similar rearrangement reaction has been reported for 1-deoxy-D-xylulose-5-phosphate reductoisomerase.[85] The hexose **13** is then converted to cPMP by formation of the pterin ring and the cyclic phosphate. Considering that MoaC binds nucleoside triphosphate stronger than di- and monophosphate,[33] the cyclic phosphate formation may be the last or close to the last step of the catalysis. Studies to further narrow the possible mechanisms are currently underway.

## CONCLUSION

This work describes the isolation and characterization of 3′,8-$cH_2$GTP, an intermediate in Moco biosynthesis, which had previously eluded structural characterization. Our finding defines the reactions catalyzed by MoaA and MoaC and provides insights into their catalytic mechanisms. In contrast to the previous notion in the field, our results suggests a complex mechanism for the MoaC-catalyzed reaction.


dx.doi.org/10.1021/ja401781t | J. Am. Chem. Soc. 2013, 135, 7019−7032

## ■ ASSOCIATED CONTENT

### Supporting Information

Detailed protocol for expression and purification of *S. aureus* MoaA and MoaC; 6-hydroxy-2,4,5-triaminopyrimidine nucleotides in the pterin and flavin biosynthesis; SDS-PAGE and UV−vis spectra of MoaA and MoaC; chromatograms of 3′,8-cH$_2$GTP purification; MS characterization of 3′,8-cH$_2$GTP; energy-minimized conformation of the nucleoside moiety of 3′,8-cH$_2$GTP; 2D NMR spectra of 3′,8-cH$_2$GTP; steady-state kinetic analysis of MoaA, MoaC, and MOCS1B; MS characterization of MOCS1B; MoaA assay with [3′-$^2$H]GTP; $^{13}$C NMR summary for purine and pyrimidine bases. This material is available free of charge via the Internet at http://pubs.acs.org.

## ■ AUTHOR INFORMATION


### Corresponding Author

ken.yoko@duke.edu


### Notes

The authors declare no competing financial interest.

## ■ ACKNOWLEDGMENTS

This work was supported by start-up funds from the Duke University Medical Center (to K.Y.), and in part by National Institutes of Health (NIH) Grant P30-CA014236 (to A.A.R.). We acknowledge the Duke University NMR Spectroscopy Center shared resource for spectrometer time. Instrumentation in the Center was purchased with support from NIH, NSF, HHMI, and the North Carolina Biotechnology Center. We thank George R. Dubay (Duke University, Department of Chemistry) for assistance on the MS measurements. We acknowledge the Duke proteomics core facility for the MS analysis of MOCS1B. We acknowledge J. A. Gerlt (University of Illinois at Urbana−Champaign) for providing an expression plasmid for 5-methylthioribose kinase, and Petra Hänzelmann and Hermann Schindelin (University of Würzburg) for providing expression plasmids for the MOCS1B and SUF proteins. We thank Dr. JoAnne Stubbe (MIT, Departments of Chemistry and Biology) for critical reading of the manuscript.

## ■ REFERENCES


(1) Hille, R.; Nishino, T.; Bittner, F. *Coord. Chem. Rev.* **2011**, *255*, 1179−1205.
(2) Hille, R. *Chem. Rev.* **1996**, *96*, 2757−2816.
(3) Johnson, J. L.; Waud, W. R.; Rajagopalan, K. V.; Duran, M.; Beemer, F. A.; Wadman, S. K. *Proc. Natl. Acad. Sci. U.S.A.* **1980**, *77*, 3715−3719.
(4) Cohen, H. J.; Fridovich, I.; Rajagopalan, K. V. *J. Biol. Chem.* **1971**, *246*, 374−382.
(5) Mendel, R. R.; Schwarz, G. *Coord. Chem. Rev.* **2011**, *255*, 1145−1158.
(6) Leimkuhler, S.; Wuebbens, M. M.; Rajagopalan, K. V. *Coord. Chem. Rev.* **2011**, *255*, 1129−1144.
(7) Wuebbens, M. M.; Rajagopalan, K. V. *J. Biol. Chem.* **1995**, *270*, 1082−1087.
(8) Wuebbens, M. M.; Rajagopalan, K. V. *J. Biol. Chem.* **1993**, *268*, 13493−13498.
(9) Hänzelmann, P.; Schindelin, H. *Proc. Natl. Acad. Sci. U.S.A* **2004**, *101*, 12870−12875.
(10) Pitterle, D. M.; Rajagopalan, K. V. *J. Bacteriol.* **1989**, *171*, 3373−3378.
(11) Pitterle, D. M.; Johnson, J. L.; Rajagopalan, K. V. *J. Biol. Chem.* **1993**, *268*, 13506−13509.
(12) Gutzke, G.; Fischer, B.; Mendel, R. R.; Schwarz, G. *J. Biol. Chem.* **2001**, *276*, 36268−36274.
(13) Nichols, J. D.; Rajagopalan, K. V. *J. Biol. Chem.* **2005**, *280*, 7817−7822.
(14) Nichols, J.; Rajagopalan, K. V. *J. Biol. Chem.* **2002**, *277*, 24995−25000.
(15) Kuper, J.; Llamas, A.; Hecht, H. J.; Mendel, R. R.; Schwarz, G. *Nature* **2004**, *430*, 803−806.
(16) Llamas, A.; Mendel, R. R.; Schwarz, G. *J. Biol. Chem.* **2004**, *279*, 55241−55246.
(17) Rieder, C.; Eisenreich, W.; O'Brien, J.; Richter, G.; Gotze, E.; Boyle, P.; Blanchard, S.; Bacher, A.; Simon, H. *Eur. J. Biochem.* **1998**, *255*, 24−36.
(18) Burg, A. W.; Brown, G. M. *J. Biol. Chem.* **1968**, *243*, 2349−2358.
(19) Fischer, M.; Bacher, A. *Chembiochem* **2011**, *12*, 670−680.
(20) Reiss, J.; Cohen, N.; Dorche, C.; Mandel, H.; Mendel, R. R.; Stallmeyer, B.; Zabot, M. T.; Dierks, T. *Nat. Genet.* **1998**, *20*, 51−53.
(21) Reiss, J.; Christensen, E.; Kurlemann, G.; Zabot, M. T.; Dorche, C. *Hum. Genet.* **1998**, *103*, 639−644.
(22) Sofia, H. J.; Chen, G.; Hetzler, B. G.; Reyes-Spindola, J. F.; Miller, N. E. *Nucleic Acids Res.* **2001**, *29*, 1097−1106.
(23) Frey, P. A.; Hegeman, A. D.; Ruzicka, F. J. *Crit. Rev. Biochem. Mol. Biol.* **2008**, *43*, 63−88.
(24) Walsby, C. J.; Hong, W.; Broderick, W. E.; Cheek, J.; Ortillo, D.; Broderick, J. B.; Hoffman, B. M. *J. Am. Chem. Soc.* **2002**, *124*, 3143−3151.
(25) Vey, J. L.; Drennan, C. L. *Chem. Rev.* **2011**, *111*, 2487−2506.
(26) Hänzelmann, P.; Schindelin, H. *Proc. Natl. Acad. Sci. U.S.A.* **2006**, *103*, 6829−6834.
(27) Lees, N. S.; Hänzelmann, P.; Hernandez, H. L.; Subramanian, S.; Schindelin, H.; Johnson, M. K.; Hoffman, B. M. *J. Am. Chem. Soc.* **2009**, *131*, 9184−9185.
(28) Zhang, Q.; Liu, W. *J. Biol. Chem.* **2011**, *286*, 30245−30252.
(29) Iobbi-Nivol, C.; Leimkuhler, S. *Biochim. Biophys. Acta* **2012**, DOI: 10.1016/j.bbabio.2012.11.007.
(30) Mehta, A. P.; Hanes, J. W.; Abdelwahed, S. H.; Hilmey, D. G.; Hänzelmann, P.; Begley, T. P. *Biochemistry* **2013**, *52*, 1134−1136.
(31) Bracher, A.; Fischer, M.; Eisenreich, W.; Ritz, H.; Schramek, N.; Boyle, P.; Gentili, P.; Huber, R.; Nar, H.; Auerbach, G.; Bacher, A. *J. Biol. Chem.* **1999**, *274*, 16727−16735.
(32) Srivastava, V. K.; Srivastava, S.; Arora, A.; Pratap, J. V. *PLoS One* **2013**, *8*, e58333.
(33) Kanaujia, S. P.; Jeyakanthan, J.; Nakagawa, N.; Balasubramaniam, S.; Shinkai, A.; Kuramitsu, S.; Yokoyama, S.; Sekar, K. *Acta Crystallogr. D: Biol. Crystallogr.* **2010**, *66*, 821−833.
(34) Wuebbens, M. M.; Liu, M. T.; Rajagopalan, K.; Schindelin, H. *Structure* **2000**, *8*, 709−718.
(35) Yoshida, H.; Yamada, M.; Kuramitsu, S.; Kamitori, S. *Acta Crystallogr. F: Struct. Biol. Cryst. Commun.* **2008**, *64*, 589−592.
(36) Hänzelmann, P.; Hernandez, H. L.; Menzel, C.; Garcia-Serres, R.; Huynh, B. H.; Johnson, M. K.; Mendel, R. R.; Schindelin, H. *J. Biol. Chem.* **2004**, *279*, 34721−34732.
(37) Hänzelmann, P.; Schwarz, G.; Mendel, R. R. *J. Biol. Chem.* **2002**, *277*, 18303−18312.
(38) Imker, H. J.; Fedorov, A. A.; Fedorov, E. V.; Almo, S. C.; Gerlt, J. A. *Biochemistry* **2007**, *46*, 4077−4089.
(39) Ames, B. N. *Methods Enzymol.* **1966**, *8*, 115−118.
(40) Edelhoch, H. *Biochemistry* **1967**, *6*, 1948−1954.
(41) Ludwig, J. *Acta Biochim. Biophys.* **1981**, *16*, 131−133.
(42) Stubbe, J.; van der Donk, W. A. *Chem. Rev.* **1998**, *98*, 705−762.
(43) Bacher, A.; Lingens, F. *J. Biol. Chem.* **1971**, *246*, 7018−7022.
(44) Cho, B. P. *Magn. Reson. Chem.* **1993**, *31*, 1048−1053.
(45) National Institute of Advanced Industrial Science and Technology, Spectral Database for Organic Compounds, http://riodb01.ibase.aist.go.jp/sdbs/ (accessed Jan 16, 2013).
(46) Weigert, F. J.; Roberts, J. D. *J. Am. Chem. Soc.* **1972**, *94*, 6021−6025.
(47) Hochlowski, J. E.; Andres, W. W.; Theriault, R. J.; Jackson, M.; McAlpine, J. B. *J. Antibiot. (Tokyo)* **1987**, *40*, 145−148.
(48) Tsunakawa, M.; Kamei, H.; Konishi, M.; Miyaki, T.; Oki, T.; Kawaguchi, H. *J. Antibiot.* **1988**, *41*, 1366−1373.

(49) Nyerges, M.; Rudas, M.; Bitter, I.; Toke, L.; Szantay, C. *Tetrahedron* **1997**, *53*, 3269−3280.
(50) Gao, X.; Chooi, Y. H.; Ames, B. D.; Wang, P.; Walsh, C. T.; Tang, Y. *J. Am. Chem. Soc.* **2011**, *133*, 2729−2741.
(51) Buttachon, S.; Chandrapatya, A.; Manoch, L.; Silva, A.; Gales, L.; Bruyere, C.; Kiss, R.; Kijjoa, A. *Tetrahedron* **2012**, *68*, 3253−3262.
(52) Dachriyanus; Sargent, M. V.; Wahyuni, F. S. *Aust. J. Chem.* **2000**, *53*, 159−160.
(53) Numata, A.; Takahashi, C.; Ito, Y.; Takada, T.; Kawai, K.; Usami, Y.; Matsumura, E.; Imachi, M.; Ito, T.; Hasegawa, T. *Tetrahedron Lett.* **1993**, *34*, 2355−2358.
(54) Lee, C. H.; Ezra, F. S.; Kondo, N. S.; Sarma, R. H.; Danyluk, S. S. *Biochemistry* **1976**, *15*, 3627−3638.
(55) Tsuboi, M.; Takahashi, S.; Kyogoku, Y.; Hayatsu, H.; Ukita, T.; Kainosho, M. *Science* **1969**, *166*, 1504−1505.
(56) Daniels, J. N.; Wuebbens, M. M.; Rajagopalan, K. V.; Schindelin, H. *Biochemistry* **2008**, *47*, 615−626.
(57) Karplus, M. *J. Chem. Phys.* **1959**, *30*, 11−15.
(58) Chatterjee, A.; Li, Y.; Zhang, Y.; Grove, T. L.; Lee, M.; Krebs, C.; Booker, S. J.; Begley, T. P.; Ealick, S. E. *Nat. Chem. Biol.* **2008**, *4*, 758−765.
(59) Yokoyama, K.; Numakura, M.; Kudo, F.; Ohmori, D.; Eguchi, T. *J. Am. Chem. Soc.* **2007**, *129*, 15147−15155.
(60) Challand, M. R.; Martins, F. T.; Roach, P. L. *J. Biol. Chem.* **2010**, *285*, 5240−5248.
(61) Bracher, A.; Schramek, N.; Bacher, A. *Biochemistry* **2001**, *40*, 7896−7902.
(62) Wuebbens, M. M.; Rajagopalan, K. V. *J. Biol. Chem.* **2003**, *278*, 14523−14532.
(63) Jung, M. E.; Choe, S. W. T. *Tetrahedron Lett.* **1993**, *30*, 6247−6250.
(64) Auerbach, G.; Herrmann, A.; Bracher, A.; Bader, G.; Gutlich, M.; Fischer, M.; Neukamm, M.; Garrido-Franco, M.; Richardson, J.; Nar, H.; Huber, R.; Bacher, A. *Proc. Natl. Acad. Sci. U.S.A.* **2000**, *97*, 13567−13572.
(65) Bracher, A.; Eisenreich, W.; Schramek, N.; Ritz, H.; Gotze, E.; Herrmann, A.; Gutlich, M.; Bacher, A. *J. Biol. Chem.* **1998**, *273*, 28132−28141.
(66) Shiota, T.; Palumbo, M. P.; Tsai, L. *J. Biol. Chem.* **1967**, *242*, 1961−1969.
(67) Weygand, F.; Wacker, H.; Dahms, G.; Schliep, H. J.; Waldschmidt, M.; Simon, H. *Angew. Chem., Int. Ed. Engl.* **1961**, *73*, 402.
(68) Nar, H.; Huber, R.; Meining, W.; Schmid, C.; Weinkauf, S.; Bacher, A. *Structure* **1995**, *3*, 459−466.
(69) Nar, H.; Huber, R.; Auerbach, G.; Fischer, M.; Hosl, C.; Ritz, H.; Bracher, A.; Meining, W.; Eberhardt, S.; Bacher, A. *Proc. Natl. Acad. Sci. U.S.A.* **1995**, *92*, 12120−12125.
(70) McCarty, R. M.; Krebs, C.; Bandarian, V. *Biochemistry* **2013**, *52*, 188−198.
(71) Grove, T. L.; Lee, K. H., St; Clair, J.; Krebs, C.; Booker, S. J. *Biochemistry* **2008**, *47*, 7523−7538.
(72) Benjdia, A.; Leprince, J.; Sandstrom, C.; Vaudry, H.; Berteau, O. *J. Am. Chem. Soc.* **2009**, *131*, 8348−8349.
(73) Padovani, D.; Thomas, F.; Trautwein, A. X.; Mulliez, E.; Fontecave, M. *Biochemistry* **2001**, *40*, 6713−6719.
(74) Cicchillo, R. M.; Iwig, D. F.; Jones, A. D.; Nesbitt, N. M.; Baleanu-Gogonea, C.; Souder, M. G.; Tu, L.; Booker, S. J. *Biochemistry* **2004**, *43*, 6378−6386.
(75) Chatgilialoglu, C.; Guerra, M.; Mulazzani, Q. G. *J. Am. Chem. Soc.* **2003**, *125*, 3839−3848.
(76) Wang, S. C.; Frey, P. A. *Biochemistry* **2007**, *46*, 12889−12895.
(77) Hinckley, G. T.; Frey, P. A. *Biochemistry* **2006**, *45*, 3219−3225.
(78) Reiss, J.; Johnson, J. L. *Hum. Mutat.* **2003**, *21*, 569−576.
(79) Reece, S. Y.; Hodgkiss, J. M.; Stubbe, J.; Nocera, D. G. *Philos. Trans. R. Soc. London B: Biol. Sci.* **2006**, *361*, 1351−1364.
(80) Dedon, P. C. *Chem. Res. Toxicol.* **2008**, *21*, 206−219.
(81) Stubbe, J.; Ackles, D. *J. Biol. Chem.* **1980**, *255*, 8027−8030.
(82) Cotruvo, J. A.; Stubbe, J. *Annu. Rev. Biochem.* **2011**, *80*, 733−767.
(83) Srivastava, S.; Srivastava, V. K.; Arora, A.; Pratap, J. V. *Acta Crystallogr. F: Struct. Biol. Cryst. Commun.* **2012**, *68*, 687−691.
(84) Alexakis, A.; Mangeney, P.; Lensen, N.; Tranchier, J. P.; Gosmini, R.; Raussou, S. *Pure Appl. Chem.* **1996**, *68*, 531−534.
(85) Munos, J. W.; Pu, X.; Mansoorabadi, S. O.; Kim, H. J.; Liu, H. W. *J. Am. Chem. Soc.* **2009**, *131*, 2048−2049.